Europäisches Patentamt
European Patent Office
Office européen des brevets

Bescheinigung Certificate Attestation

Die angehefteten Unterlagen stimmen mit der ursprünglich eingereichten Fassung der auf dem nächsten Blatt bezeichneten europäischen Patentanmeldung überein.

The attached documents are exact copies of the European patent application described on the following page, as originally filed.

Les documents fixés à cette attestation sont conformes à la version initialement déposée de la demande de brevet européen spécifiée à la page suivante.

Patentanmeldung Nr. Patent application No. Demande de brevet n°

02011074.8

PRIORITY DOCUMENT
SUBMITTED OR TRANSMITTED IN COMPLIANCE WITH RULE 17.1(a) OR (b)

Der Präsident des Europäischen Patentamts;
Im Auftrag

For the President of the European Patent Office

Le Président de l'Office européen des brevets
p.o.

R C van Dijk

Anmeldung Nr:
Application no.: 02011074.8
Demande no:

Anmeldetag:
Date of filing: 17.05.02
Date de dépôt:

Anmelder/Applicant(s)/Demandeur(s):

Strebhardt, Klaus, Prof. Dr.
Biedenkopfer Weg 24
60489 Frankfurt
ALLEMAGNE

Bezeichnung der Erfindung/Title of the invention/Titre de l'invention:
(Falls die Bezeichnung der Erfindung nicht angegeben ist, siehe Beschreibung.
If no title is shown please refer to the description.
Si aucun titre n'est indiqué se referer à la description.)

Inhibition of proliferative diseases by agents which are directed against PLK1 and are selected from antisense oligonucleotides, duplex RNAs and inhibitory peptides

In Anspruch genommene Priorität(en) / Priority(ies) claimed /Priorité(s) revendiquée(s)
Staat/Tag/Aktenzeichen/State/Date/File no./Pays/Date/Numéro de dépôt:

EP/22.02.02/EP 02003982

Internationale Patentklassifikation/International Patent Classification/
Classification internationale des brevets:

A61K48/00

Am Anmeldetag benannte Vertragstaaten/Contracting states designated at date of filing/Etats contractants désignées lors du dépôt:

AT BE CH CY DE DK ES FI FR GB GR IE IT LI LU MC NL PT SE TR

WEICKMANN & WEICKMANN

Patentanwälte
European Patent Attorneys · European Trademark Attorneys

DIPL.-ING. H. WEICKMANN (bis 31.1.01)
DIPL.-ING. F. A. WEICKMANN
DIPL.-CHEM. B. HUBER
DR.-ING. H. LISKA
DIPL.-PHYS. DR. J. PRECHTEL
DIPL.-CHEM. DR. B. BÖHM
DIPL.-CHEM. DR. W. WEISS
DIPL.-PHYS. DR. J. TIESMEYER
DIPL.-PHYS. DR. M. HERZOG
DIPL.-PHYS. B. RUTTENSPERGER
DIPL.-PHYS. DR.-ING. V. JORDAN
DIPL.-CHEM. DR. M. DEY
DIPL.-FORSTW. DR. J. LACHNIT

Unser Zeichen:
27492P EP-1/BBcl

Anmelder:
Prof. Dr.
Klaus Strebhardt
Biedenkopfer Weg 24

60489 Frankfurt
DEUTSCHLAND

Inhibition of proliferative diseases by agents which are directed against PLK1 and are selected from antisense oligonucleotides, duplex RNAs and inhibitory peptides

---

Postfach 860 820, 81635 München, Deutschland. Tel. (089) 45563 0 Fax (089) 45563 999 email@weickmann.de

Inhibition of proliferative diseases by agents which are directed against PLK1 and are selected from antisense-oligonucleotides, duplex RNAs and inhibitory peptides.

Specification

In eukaryotes, double-stranded (ds) RNA induces sequence-specific inhibition of gene expression referred to as RNA interference (RNAi). Since PLK1 (polo-like kinase 1) expression is elevated in a broad range of human tumors, RNAi was exploited to define the role of PLK1 for neoplastic proliferation.

After transfection Northern and Western blot analyses were used to examine the potential of 21-nt-long, short interfering (si) duplex RNAs targeted against human PLK1 for specific inhibition of PLK1 gene expression. Furthermore, the influence of dsRNAs on the phenotype and the proliferation of cancer cells was monitored.

Treatment of cancer cell lines (MCF-7 breast, HeLa S3 cervix, SW-480 colon and A549 lung) with appropriate dsRNAs resulted in a sequence-specific decrease in the level of mRNA and protein expressed from the human PLK1-gene. The analysis of mitotically arrested SW480 cells by fluorescence microscopy revealed centrosomes that lost their ability for microtubule nucleation. Moreover, dsRNA treatment against PLK1 resulted in a potent antiproliferative effect and apoptosis in tumor cells of different origin consistent with a powerful RNA silencing effect for the applied dsRNAs. In contrast, primary mammary epithelial cells exhibited low sensitivity towards PLK1-specific dsRNA. All statistical tests were two-sided.

These data indicate that PLK1 function is essential for

centrosome-mediated microtubule events and consequently for spindle assembly. Our observations implicate that dsRNAs targeted against human PLK1 may be valuable tools as antiproliferative agents that display activity against a broad spectrum of neoplastic cells at very low doses.

RNA-interference (RNAi) as part of a primitive immune system represents the ability of some viruses, transgenes or RNAs to trigger post-transcriptional degradation of homologous cellular RNAs (1,2). This mechanism has evolved to protect the genome of an organism against the hostile environment with dangerous opportunities for unwanted gene expression and with parasites (transposons and viruses). Double-stranded RNA (dsRNA) has been shown to trigger sequence-specific gene silencing in numerous organisms such as nematodes, plants, trypanosomes, fruit flies and planaria. Studies in C. *elegans* and Drosophila revealed that a few molecules per cell are sufficient to eliminate a much larger pool of endogenous mRNA and thereby induce a strong RNAi response suggesting a catalytic or amplification mechanism to contribute to gene silencing (3,4). After selection of a specific mRNA as target for RNAi, endogenous cleavage is a key step in degradation of the target mRNA. In Drosophila RNAi is independent of mRNA translation but requires ATP (5). During this process dsRNA is reduced in size to fragments of 21-23 nucleotides by a ribonuclease III protein that is independent of the targeted mRNA. Subsequent cleavage of the mRNA was observed only within the region of identity with the dsRNA. In a recent study RNA duplexes of 21 nucleotides in length were shown to suppress gene expression in mammalian cell lines (6). This report suggested that longer dsRNAs (50- and 500-bp) induced nonspecific reduction in reporter-gene expression probably as part of an interferon response (7).

Increasing knowledge about the genetic control of cellular proliferation provides the basis for the rational design of specific therapeutic strategies aimed at the regulation of proliferative disorders such as cancer. A key

regulator for the mitotic progression in mammalian cells is the polo-like kinase (PLK1) which is structurally related to the polo gene product of Drosophila melanogaster, Cdc5p of Saccharomyces cerevisiae and plo1$^+$ of Schizosaccharomyces pombe (8). The plks from yeast, insects, amphibians and mammals represent a group of serine/threonine kinases that share a high degree of homology suggesting that the proteins have a close evolutionary and thereby functional relationship. PLK1 activity is elevated in tissues and cells exhibiting a high mitotic index including tumors (9,10). An increasing body of evidence suggests that the frequency of PLK1 expression is of prognostic value for patients suffering from different types of tumors like non-small cell lung cancer, squarnous cell carcinomas of head and neck, melanomas, oropharyngeal carcinomas, ovarian and endometrial carcinomas (11). The importance of PLK1 as measure for the aggressiveness of a tumor results from its leading role for mitotic progression in particular the G_2/M transition (control of the mitosis promoting factor) (12). Moreover, PLK1 controls also additional steps during mitotic progression: regulation of the anaphase promoting complex and cytokinesis (13-15). Considering the potency of dsRNA for sequence-specific mRNA degradation in insect cells and the key role of PLK1 for mitosis, the current study focused on the inhibition of PLK1 expression in human cancer cells by RNA interference.

It was, therefore, an object of the present invention to provide a possibility to inhibit PLK1 activity.

In a first aspect of the present invention, this problem was solved by providing dsRNAs which are directed against PLK1 and their use for inhibiting PLK1 activity in the treatment of proliferative diseases and especially cancer diseases.

dsRNAs and antibodies

dsRNAs were synthesized and purified by Dharmacon Research Inc. (Colorado, USA). The dsRNA sequences targeting PLK1 (NCBI accession number: X75932) correspond to positions 178-200 (dsRNA2), 362-384 (dsRNA3), 1416-1438 (dsRNA4) and 1570-1572 (dsRNA5) located within the open reading frame. dsRNA1 directed against lamin A/C (NCBI accession number: X03444) represents positions 608-630 relative to the start codon. Such dsRNAs as well as their use for the treatment of proliferative disorders are considered especially preferred embodiments of the present invention.

The control dsRNA (scrambled) corresponds to the base composition of dsRNA4 as random sequence. Monoclonal PLK1 antibodies were obtained from Transduction Laboratories (Heidelberg) for Western blots and from Zytomed (San Francisco, USA) for kinase assays. Antibodies for actin were purchased from Sigma (Deisenhofen).

RNA preparation and Northern Blots

For isolation of total RNA an RNeasy-kit was used according to the manufacturer's protocol (Qiagen, Hilden). Radiolabeling of probes for PLK1 and ß-actin was performed using 250 μCi of [α-P^{32}]dCTP (6000 Ci/mmol; 1Ci = 37 GBq) for each reaction, 50 μM of each other dNTP and 10 pmol (each) of primer PLK1-17-low (5'-tgatgttggcacccttcagc-3') or actin-2-low (5'-catgaggtagtcagtcaggtc-3') as described previously (16). Northern blotting and hybridizations were carried out as reported (17).

Cell Culture

Ham's F12 and FCS were purchased from PAA, DMEM, RPMI 1640, PBS, OPTIMEM, oligofectamine, glutamine, penicillin/streptomycin and trypsin from Invitrogen (Karlsruhe). Tumor cell lines SW-480, MCF-7 and HeLa S3 were provided by DSMZ (Braunschweig) and A549 by CLS (Heidelberg).

Mammary epithelial basal medium (MEBM), growth medium supplements (MEGM Single quots) and the normal mammary epithelial cell system (HMEC) established from normal breast tissue were obtained from Clonetics (Verviers, Belgium). HMECs were passaged to select desired cells and cryopreserved in sixth passage, assured for fifteen population doublings by the manufacturer. Cell culture was performed according to the supplier's instructions.

Western Blot Analysis

48 hrs after dsRNA treatment cells were lysed for subsequent Western blotting (16). Membranes were kept for 1 hr with monoclonal antibodies for PLK1 (1:250) and actin (1:200.000) followed by incubation with goat anti-mouse serum (1:2.000) for 30 min. Western blots were performed as described (18).

Kinase Assays

48 hrs after dsRNA treatment cells were lysed, endogenous PLK1 was immunoprecipitated using monoclonal PLK1 antibodies, incubated with 0.5-1 μg of substrate and 2 μCi of [γ-P^{32}]ATP for 30 min at 37°C in kinase buffer (20 mM HEPES pH 7.4, 150 mM KCl, 10 mm $MgCl_2$, 1 mM EGTA, 0.5 mM DTT, 5 mM NaF, 0.1 mM Na_3VO_4) and products of kinase reaction were fractionated on a 12% SDS-polyacrylamid gel (BioRad, München).

Indirect Immunofluorescence

Cells were stained as described before (18). Antibodies were used as follows: polyclonal rat α-tubulin (Serotec/Biozol, Eching) 1:100, polyclonal rabbit PLK1 (19) 1:100 or monoclonal γ-tubulin (Sigma) 1:100. Cells were analyzed with a confocal laser scan microscope (CLSM) using a 100x oil immersion objective.

FACS analysis

Analysis of cell cycle and apoptosis was carried out using a Becton Dickinson FACScan. Cells were harvested, washed with PBS and probed with CycleTEST™ PLUS DNA reagent kit (Becton Dickinson) according to the manufacturer's protocol. For apoptosis detection cells were harvested 48 hrs after transfection, fixed with ice-cold 70% ethanol, treated with RNase A (5 µg/ml) and stained with propidium iodide (50 µg/ml). Subsequent analyses were performed using the CELLQuest software.

In vitro administration of dsRNAs and determination of cell proliferation

After transfection of cancer cells (oligofectamine method) the inhibitory activity of dsRNA1-5 on cell proliferation was tested. In brief, 1 day before transfection cells were split to a density of $5x10^5$ /25cm^2-culture flask corresponding to a density of 40-50% at the time of transfection. Cells were treated with dsRNA2-5 (PLK1) or dsRNA1 (lamin) as internal negative control at a concentration of 56 nM or in the dose-dependence experiments with concentrations of 0.5 nM-2 µM. Incubation with dsRNAs in OPTIMEM with oligofectamine at 37°C for 4 hrs was followed by addition of fresh medium with threefold FCS. At the appropriate time after dsRNA treatment cell numbers were determined using a hemacytometer. Cell viability was assessed by trypan blue staining. Each experiment was performed in triplicate and the standard deviation for each group was determined.

Quantitative analysis

Quantification of PLK1 and actin levels was performed using a Kodak gel documentation system (ID 3.5). To determine Northern and Western blot signal intensities, autoradiographs were scanned. Integration of signal intensities was followed by quantitative comparison of PLK1 and actin

expression. The expression values were given in percentage of control.

Statistical methods

Statistical analysis was performed with two-sided paired t-test and p-values were calculated compared to untreated control.

dsRNAs inhibit the expression of PLK1 mRNA and protein specifically

Because RNAi acts by decreasing the half-life of RNA, the natural stability of RNA will have a quantitative influence upon its suitability as target for gene silencing. Thus, we started our study by testing dsRNAs for their ability to reduce the endogenous level of PLK1 mRNA in different cancer cell lines (MCF-7 breast, HeLa S3 cervix, SW-480 colon and A549 lung). Four duplex RNAs, each 21-nt in length (dsRNA2-5) with symmetric 3' overhangs of 2 deoxythymidines, directed against the open reading frame of PLK1 were tested for their potential of PLK1-specific interference in tumor cells. As an internal negative control a duplex RNA targeted against lamin (dsRNA1) was used. Northern blot analyses standardized to the expression of actin were performed. Treatment of MCF-7 breast cancer cells in vitro with dsRNA2-5 at a concentration of 56 nM in the presence of oligofectamine did not reduce PLK1 mRNA 6 hrs after transfection significantly but led to an essential loss of PLK1 mRNA within 24 hrs and 48 hrs (Fig. 1 A). The study revealed that all tested dsRNAs targeted against PLK1 led to reduced PLK1 mRNA levels in human MCF-7 cells to levels of 20-30% compared to untreated cells. Suppression by dsRNA2-5 could not only be demonstrated for MCF-7 cells but also for other tumor cell types like HeLa S3 and SW-480 (Fig. 1 B, C). In SW-480 cells the reduction of PLK1 mRNA occurred rather rapidly within 6 hrs but was only apparent for dsRNA4 and dsRNA5. Suppression by dsRNA4 was also observed in A549 cells (Fig. 1 D).

Subsequently, we determined whether decreases in PLK1 mRNA were accompanied by corresponding reduction of PLK1 protein. The expression of PLK1 protein in different tumor cell lines was evaluated 48 hrs after single application of dsRNAs. Significant inhibition ($p<0.001$) of the 68 kDa-PLK1 protein in MCF-7 cells was observed with dsRNA4 and dsRNA5 (87 and 79%, respectively), which were previously shown to reduce PLK1 transcript levels significantly (Figs. 1A, 2A). A reduction of PLK1 mRNA induced by the application of dsRNA3-5 correlated also to a significantly lower level of the corresponding protein in HeLa S3 (dsRNA3: 81%; $p<0.001$; dsRNA4: 65% and dsRNA5: 73%; $p<0.01$), SW-480 (dsRNA4: 82% and dsRNA5: 92%; $p<0.001$) and A549 cells (dsRNA3: 70%; $p<0.01$; dsRNA4: 84% and dsRNA5: 6[illegible]%; $p<0.001$) (Fig. 2B-D).

To test for the specificity of the dsRNA action, dsRNA1 (control) directed against lamin was evaluated for its potential to alter expression of PLK1 or actin. The levels (mRNA, protein) were not influenced significantly proposing that the above described effects on cells treated with dsRNAs are sequence-specific for PLK1. This notion gained further support from the observation that dsRNA2-5 did not alter the expression of actin mRNA either. Furthermore, the concentration of dsRNA4 correlated to protein levels of PLK1 (Fig. 2E). The treatment of MCF-7 cells with dsRNA4 at concentrations between 5.6 and 56 nM exhibited a pronounced inhibitory effect on PLK1 protein levels (inhibition of 81%). Increasing the concentration to 566 nM diminished the inhibitory potential of dsRNA4. On the other hand reducing the concentration to 0.5 nM did not increase the level of PLK1 protein.

Immunoprecipitated PLK1 from MCF-7 cells treated with dsRNA for 48 hrs was subjected to kinase assays to directly assess whether downregulation of PLK1 protein level correlates also to reduced PLK1 kinase activity. In dsRNA4-treated cells phosphorylation of the cytoplasmic retention signal within human cyclin B1 as exogenous substrate (12) was reduced to 18%

of the level in control cells (data not shown). Taken together, these results suggest that PLK1 mRNA and protein were specifically reduced in dsRNA-treated cancer cells correlating with low levels of PLK1 activity.

Reduced levels of PLK1 protein result in abrogation of spindle formation

In previous studies microinjection of PLK1-specific antibodies induced abnormal distribution of condensed chromatin and monoastral microtubule arrays that were nucleated from duplicated but unseparated chromosomes (20). Here we focused on analyzing the phenotype of dsRNA-treated cells that exhibit a major downregulation of PLK1 expression in cancer cells. Antibodies directed against α-tubulin to visualize the spindle apparatus and γ-tubulin to localize centrosomes were used for staining 48 hrs after transfection. While untreated control cells proceeded through mitosis, cells incubated with dsRNA4 arrested in different mitotic stages depending on the cell type. SW-480 cells treated with dsRNA4 did not enter prophase as can be derived from the lack of prophase typical chromosome condensation in the nuclei of DAPI-stained cells. However, many cells were found with separated centrosomes which moved to opposite ends of the nucleus (Fig. 3A upper panel; γ-tubulin). Centrosomes were devoid of any microtubule connection (Fig. 3A upper panel; α-tubulin). According to their DAPI-fluorescence nuclei contained 4N DNA although no chromatin condensation was detected. Thus, while the centrosomes performed prophase-typical separation, nuclei seem to persist in G2-phase. For comparison, in untreated controls centrioles in this early state of prophase organized astral microtubules (Fig. 3A lower panel) and displayed chromosome condensation in the nucleus.

MCF-7 cells on the other hand displayed numerous apoptotic nuclei in DAPI-stained cultures but no mitotic stages after dsRNA4 treatment. Examination of the supernatant of these cultures revealed a high percentage of mitotic cells which obviously lost substrate adhesion.

Metaphase or telophase chromosomal arrangements were rarely identified. More than 90% of all mitotic stages were characterized by highly condensed, knob-like chromosomes which remained in an overall structure resembling the shape of a nucleus (Fig. 3B). Only a few chromosomes left this ensemble lying in the immediate vicinity. This phenotype indicates that the nuclear envelope has disappeared but no further, mitotic spindlerelated arrangement of chromosomes occurred. Chromatid separation did not take place. *γ*-tubulin was distributed all over the cytoplasm of these cells which also did not contain any microtubules. The lack of microtubules could be a consequence of cell death after loss of adhesion. In contrast, primary epithelial cells (HMEC treated with dsRNA4 at the same concentration proceeded through mitosis with normal phenotype.

dsRNA treatment induces G_2/M cell cycle arrest and apoptosis in cancer cells in vitro

FACScan-analysis was performed to determine the role of cell cycle arrest for the death of dsRNA-treated cells. A strong G_2/M arrest was detected: SW-480 (fivefold), MCF-7 (threefold), HeLa S3 (fivefold) and A549 cells (twofold) (Fig. 4A). CLSM experiments revealed an elevated number of apoptotic cells with disintegrated nuclear membranes and condensed chromatin (Fig. 4B). To address this observation in more detail, we asked the question whether gene silencing of PLK1 causes apoptosis in different tumor types. The percentage increase of Sub2N DNA content was determined with FACScan analysis. While control cells exhibited between 1 and 5% Sub2N DNA, PLK1-specific dsRNA4 induced increased Sub2N DNA in SW-480 (17%), MCF-7 (33%), HeLa S3 (50%) and A549 cells (13%) 48 hrs after transfection. This phenomenon can be explained with activation of interferones because dsRNAs are known to induce IFN*α/β* and to be pro-apoptotic agents (7).

Furthermore, the sensitivity of primary human mammary epithelial cells

(HMEC) towards dsRNAs was evaluated. In contrast to the cancer cells tested, primary cells did not exhibit G_2/M arrest after treatment with 56 nM dsRNA4. dsRNAs did not induce an apoptotic phenotype and did not increase the ratio of Sub2N DNA significantly suggesting a differential effect of dsRNA in cancer cells compared to normal cells.

PLK1-specific dsRNAs inhibit the growth of cancer cells in vitro

MCF-7 cells were treated with dsRNAI-5 at a concentration of 56 nM to determine whether dsRNAs influence the proliferation of tumor cells. The growth rate of $5x10^5$ cells was determined over a period of four days. While the treatment with the transfection agent (oligofectaniine) alone had no effect on the growth rate of MCF-7 cells, treatment with a control dsRNA1 (lamin) had only limited effect (Fig. 5A). In contrast, dsRNA2-5 had a significant antiproliferative effect compared to untreated MCF-7 cells within 96 hrs (dsRNA2: 83%; $p<0.01$; dsRNA3: 81%; dsRNA4: 97%; dsRNA5: 89%; $p<0.001$ for dsRNA3-5) (Fig. 5A). Specificity of the dsRNA-mediated inhibition was also indicated by a dose-dependent reduction of cell growth (Fig. 5B). Treating MCF-7 cells with dsRNA1 (lamin) or with a scrambled control dsRNA demonstrated that both dsRNAs did not reduce cell numbers significantly in any concentration tested compared to oligolectamine. In contrast, increasing concentrations of dsRNA4 (5.6-566 nM) led after 48 hrs to almost complete cell death (Fig. 5B). It was subsequently examined whether the reduction of proliferative activity is cell type-specific or can also be achieved in other cancer cell lines. dsRNA4 and dsRNA5 were shown to inhibit cell growth also significantly in SW-480 ($p<0.01$), HeLa S3 ($p<0.001$) and in A549 cells ($p<0.05$) suggesting that PLK1 expression is essential for the proliferation of different types of cancer cells (Fig. 5C-E).

Subsequently, the growth behavior of the tumor cell line MCF-7 was compared to normal mammary epithelial cells (HMEC). To gain the same

extent of growth reduction in primary epithelial cells (HMEC), a 350fold higher concentration of dsRNA4 was required compared to MCF-7 cancer cells. While in MCF-7 cells a growth reduction of 38% could be achieved with a dsRNA4 concentration of 5.6 nM, in HMECs for a growth reduction of 31% 2 μM were required (Fig. 5F). This observation suggested an elevated sensitivity of cancer cells towards dsRNA directed against PLK1 compared to primary epithelial cells.

Recent observations shed light on double-stranded RNA as a tool for the 'knock-down' of gene expression in a number of organisms (1,2). RNAi seems to be important for many developmental and antiviral mechanisms. Still, the analysis of RNAi in C. elegans revealed target RNAs that partially or fully resist post-transcriptional gene silencing (16). While reduction of reporter gene expression in Drosophila S2 cells was almost complete, specific suppression in mammalian cells was either less pronounced or could not be achieved (6). These observations raised the question whether RNA silencing is a general phenomenon in mammalian cells. Thus, the purpose of the present study was to explore the potential use of duplex RNAs for the inhibition of human cancer cells. In addition, we intended to evaluate the role of PLK1 for the proliferation of tumor cells. Our study demonstrated that administration of dsRNAs targeted against human PLK1 reduced the level of PLK1 transcripts in cell culture. dsRNA4 exhibited a pronounced inhibitory effect at a concentration of 5.6 nM. The effect disappeared if the dsRNA concentration was reduced below 0.5 nM. One of the most attractive features of dsRNA-based gene silencing is the potent inhibitory effect at low concentrations. In comparison, phosphorothioate antisense oligonucleotides display IC50 values between 100 and 500 nM (21). Thus, the limitation of phosphorothioate antisense oligonucleotides as pharmacological agent due to the potential toxicity seems to be less likely in the case of dsRNA, because efficient 'knock-down' of target genes can be achieved with very low concentrations. Moreover, we paid considerable attention to the specificity of administered dsRNA. First, within a small set

of tested dsRNAs targeted to different regions of human PLK1 only certain candidates had a potent silencing effect. Since the mechanism of RNA silencing is still under vivid investigation, we assume that silencing efficiency could reflect several parameters such as tissue-specific effects, RNA stability and homeostatic regulation, which can answer a decrease in mRNA concentration with a metabolic compensation that would restore expression levels. Second, a scrambled dsRNA (permutated sequence of dsRNA4) or a dsRNA targeted to lamin had only little effect on the level of PLK1 mRNA. Non-specific reduction of mRNA expression was expected as part of the interferon response in living cells (7). Four tumor cell types were responsive to the antiproliferative effects of dsRNA4 (MCF-7 breast, HeLa S3 cervix, SW-480 colon and A549 lung), supporting the premise that PLK1 silencing might be useful for the treatment of tumors in future in vivo experiments. This view gained attractive support by the observation that primary epithelial cells were not suppressed by dsRNA at concentrations that extinguished tumor cells. Thus, toxic side-effects in normal cells exerted by dsRNA targeted to human PLK1 are less likely. Taken together, these observations strongly suggest that the inhibitory effect of dsRNA4 on PLK1 expression and the biological consequences that appear to result from these inhibitory effects in cell culture occur through an RNA silencing mechanism.

The ability to use duplex RNA to target selectively genetic mechanisms involved in tumorigenesis gives rise to the fascinating chance that these novel agents could be used, not only as a new class of chemotherapeutic agents to combat cancer, but also to gain a better understanding of the critical molecular events responsible for initiating and maintaining the cancer phenotype. The above results raise some intriguing questions relative to the role of PLK1 in cancer cells. Centrosomes play a critical role in generating genetic instability in cancer cells (22,23). They contribute to spindle abnormalities and disturbed chromosome segregation, which is often accompanied with profound alterations in key cellular functions like

apoptosis, cell cycle progression, control of cell cycle checkpoints and cell growth regulation. Different studies tested the impact of PLK1 on the function of mammalian centrosomes (20,23-25). While the analysis of HeLa cells microinjected with PLK1-specific antibodies revealed monoastral microtubule arrays that were nucleated from duplicated but unseparated centrosomes, RNA silencing allowed to separate centrosome division from microtubule anchoring: Centrosomes still divided and separated from each other but obviously without microtubule interaction. If the pericentriolar matrix surrounding centrioles becomes dissolved in early prophase, centrosomes are not kept in close proximity any longer. Lack of PLK1 after dsRNA treatment prevents the formation of the microtubule nucleation complex required for aster and spindle formation.

In MCF-7 cells centrioles could not organize microtubules because chromosome arrangements other than those typical for late interphase/early prophase nuclei are very rare. While SW-480 cells arrest predominantly in G_2/prophase, MCF-7 cells proceed further to pro-/prometaphase characterized by condensed chromosomes and beginning nuclear envelop breakdown. This phenotype is a consequence of missing spindle formation and retarded chromosome separation (26). Thus, 'knock-down' of PLK1-function may induce different mitotic phenotypes at various stages due to varying checkpoint control in different cancer cells or might alternatively correlate to the endogenous level of PLK1 mRNA in tumor cells reflecting a mutation-sensitive interaction of PLK1 mRNA and Hsp90 (27).

Taken together, although, the mammalian genome contains several polo-related kinases, the 'knock-down' of PLK1 alone by RNA silencing is sufficient to prevent centrosome-induced spindle formation and to induce apoptosis in different tumor cells. Extra centrosomes in cancer cells might lead to chromosome missorting and damage causing aneuploidy which may induce the loss of tumor suppressor genes or activate oncogenes. Recent

observations pointed out that centrosomal abnormalities can be detected in early forms of human breast and prostate cancer (28). This might suggest that centrosomes are the driving force of cancer formation instead of being a consequence of it. Our cell culture experiments indicate that gene silencing of PLK1 inhibits centrosome fimction to an extent which induces apoptosis of cancer cells. Future experiments might also shed fight on new techniques aimed at restoring normal centrosome function by regulating PLK1 activity. Furthermore, investigations examining the effects of dsRNA4 against tumors in Xenograft experiments are of obvious importance.

REFERENCES

(1) Sharp PA. RNA interference--2001. Genes Dev 2001; 15:485-490.

(2) Fire A. RNA-triggered gene silencing. Trends Genet 1999; 15:358-363.

(3) Fire A, Xu S, Montgomery MK, Kostas SA, Driver SE, and Mello CC. Potent and specific genetic interference by double-stranded RNA in Caenorhabditis elegans. Nature 1998;391:806-811.

(4) Montgomery MK, Xu S, and Fire A. RNA as a target of double-stranded RNA-mediated genetic interference in Caenorhabditis elegans. Proc Natl Acad Sci U S A 1998;95:15502-15507.

(5) Zamore PD, Tuschl T, Sharp PA, and Bartel DP. RNAi: double-stranded RNA directs the ATP-dependent cleavage of mRNA at 21 to 23 nucleotide intervals. Cell 2000;101:25-33.

(6) Elbashir SM, Harborth J, Lendeckel W, Yalcin A, Weber K, and Tuschl T. Duplexes of 21-nucleotide RNAs mediate RNA interference in cultured mammalian cells. Nature 2001;411:494-498.

(7) Der SD, Yang YL, Weissmann C, and Williams BR. A double-stranded RNA-activated protein kinasedependent pathway mediating stress-induced apoptosis. Proc Nad Acad Sci U S A 1997;94:3279-3283.

(8) Glover DM, Hagan IM, and Tavares AA. Polo-like kinases: a team that plays throughout mitosis. Genes Dev 1998;12:3777-3787.

(9) Golsteyn RM, Schultz SJ, Bartek J, Ziemiecki A, Ried T, and Nigg EA. Cell cycle analysis and chromosomal localization of human PIK1, a putative homologue of the mitotic kinases Drosophila polo and Saccharomyces cerevisiae Cdc5. J Cell Sci 1994; 107 (Pt 6):1509-1517.

(10) Holtrich U, Wolf 6, Brauninger A, Karn T, Bohme B, Rubsamen-Waigmann H et al. Induction and downregulation of PLK, a human serine/threonine kinase expressed in proliferating cells and tumors. Proc Natl Acad Sci U S A 1994;91:1736-1740.

(11) Strebhardt K. PLK (polo-like kinase). In: Creighton TE, editor. Encyclopedia of Molecular Medicine. New York, N.Y.: Wiley and Sons, Inc.; 2001. p. 2530-2332.

(12) Toyoshima-Morimoto F, Taniguchi E, Shinya N, Iwamatsu A, and Nishida E. Polo-like kinase I phosphorylates cyclin B I and targets it to the nucleus during prophase. Nature 2001;410:215-220.

(13) Qian YW, Erikson E, Taieb FE, and Mailer JL. The polo-like kinase Plx I is required for activation of the phosphatase Cdc25C and cyclin B-Cdc2 in Xenopus oocytes. Mol Biol Cell 2001;12:1791-1799.

(14) Shirayama M, Zachariae W, Ciosk R, and Nasmyth K. The Polo-like kinase Cdc5p and the WD-repeat protein Cdc20p/fizzy are regulators and substrates of the anaphase promoting complex in Saccharomyces cerevisiae. EMBO J 1998;17:1336-1349.

(15) Ohkura H, Hagan IM, and Glover DM. The conserved Schizosaccharomyces pombe kinase plo I, required to form a bipolar spindle, the actin ring, and septum, can drive septum formation in G 1and G2 cells. Genes Dev 1995;9:1059-1073.

(16) Hock B, Bohme B, Karn T, Yamamoto T, Kaibuchi K, Holtrich U et al. PDZ-domain-mediated interaction of the Eph-related receptor tyrosine kinase EphB3 and the ras-binding protein AF6 depends on the kinase activity of the receptor. Proc Natl Acad Sci U S A 1998;95:9779-9784.

(17) Wolf G, Elez R, Doermer A, Holtrich U, Ackermann H, Stutte HJ et al. Prognostic significance of pololike kinase (PLK) expression in non-small cell lung cancer. Oncogene 1997; 14:543-549.

(18) Kauselmann G, Weiler M, Wulff P, Jessberger S, Konietzko U, Scafidi J et al. The polo-like protein kinases Fnk and Snk associate with a Ca(2+)- and integrin-binding protein and are regulated dynamically with synaptic plasticity. EMBO J 1999; 18:5528-5539.

(19) Yuan J, Horlin A, Hock B, Stutte HJ, Rubsamen-Waigmann H, and Strebhardt K. Polo-like kinase, a novel marker for cellular proliferation. Am J Pathol 1997; 150:1165-1172.

(20) Lane HA and Nigg EA. Antibody microinjection reveals an essential role for human polo-like kinase I (Pik 1) in the functional maturation of mitotic centrosomes. J Cell Biol 1996; 135:1701-1713.

(21) Tamm I, Dorken B, and Hartmann G. Antisense therapy in oncology: new hope for an old idea? Lancet 2001;358:489-497.

(22) Brinkley BR. Managing the centrosome numbers game: from chaos to stability in cancer cell division. Trends Cell Biol 2001; 11: 18-21.

(23) Doxsey SJ. Re-evaluating centrosome function. Nat Rev 2001;2:688-698.

(24) Cogswell JP, Brown CE, Bisi JE, and Neill SD. Dominant-negative polo-like kinase I induces mitotic catastrophe independent of cdc25C function. Cell Growth Differ 2000;11:615-623.

(25) do Carmo AM, Tavares A, and Glover DM. Polo kinase and Asp are needed to promote the mitotic organizing activity of centrosomes. Nat Cell Biol 200 1;3:421-424.

(26) Alexandru G, Uhlmann F, Mechtler K, Poupart MA, and Nasmyth K. Phosphorylation of the cohesin subunit Scc1 by Polo/Cdc5 kinase regulates sister chromatid separation in yeast. Cell 2001;105:459-472.

(27) Simizu S and Osada H. Mutations in the Pik gene lead to instability of Pik protein in human tumour cell lines. Nat Cell Biol 2000;2:852-854.

(28) Pihan GA, Purohit A, Wallace J, Malhotra R, Liotta L, and Doxsey SJ. Centrosome defects can account for cellular and genetic changes that characterize prostate cancer progression. Cancer Res 2001;61:2212-2219.

FIGURE LEGENDS

Fig. 1. Reduction of PLK1 mRNA in cancer cells. (A) Northern blot analysis of PLK1 mRNA in MCF-7 cells 6, 24 and 48 hrs after dsRNA treatment. To ascertain uniformity of loading membranes were reprobed with human β-actin. Indicated are signals for PLK1 and actin in all autoradiographs. Percent inhibition was calculated by comparison with PLK1 mRNA levels of cells grown in the absence of dsRNAs. PLK1 mRNA expression in HeLa S3 (B), SW-480 (C) and A549 cells (D) 6, 24 and 48 hrs after dsRNA application.

Fig. 2. Inhibition of PLK1 protein expression by PLK1-specific dsRNAs. Percent inhibition was calculated by comparison with PLK1 protein levels in cells grown in the absence of dsRNAs. (A) Western blot analysis of PLK1 protein in MCF-7 cells 48 hrs after dsRNA treatment. Indicated are the signals for PLK1 and actin. Actin served as control for equal loading (upper panel). Mean values of at least 3 independent experiments with standard deviation are shown (lower panel). Quantification of PLK1 protein in HeLa S3 cells (B), SW480 cells (C) and A549 cells (D) after normalization to actin. (E) PLK1 protein correlated to the concentration of dsRNA4 in MCF-7 cells.

Fig. 3. dsRNA4 treatment resulted in abrogated spindle formation at centrosornes in SW-480 cells and disturbed chromosome phenotypes in early mitosis of MCF-7 cells. Cells were transfected with dsRNA4 and immunostained 48 hrs post transfection for y- (green), α-tubulin (red) and DAPI (blue). (A) dsRNA4-treated SW-480 cells with missing spindles at centrosomes. (upper panel); arrows: cell with centrosomes devoid of any mikrotubule connection; untreated cells with normal spindle formation (lower panel). (B) Supernatant of MCF-7 cell cultures treated with dsRNA4 contained many mitotic cells. Most of them were characterized by highly

condensed, knob like chromosomes. Some chromosomes are located adjacent to the nucleus (arrows).

Fig. 4. dsRNA treatment induced G_2/M cell cycle arrest and apoptosis in cancer cells. (A) FACScan analysis demonstrated strong G_2/M arrest in SW-480, MCF-7, HeLa S3 and A549 cells. (B) Confocal laser scanning microscopy revealed apoptotic cells with disintegrated nuclear membranes and condensed chromatin (phase contrast image).

Fig. 5. Antiproliferative effects of PLK1-specific dsRNA-mediated inhibition in cancer cells. dsRNA against lamin served as internal negative control. Percent inhibition was calculated by comparison to the number of cells grown in the absence of dsRNAs. (A) Growth inhibition of MCF-7 cells over a period of 4 days. (B) Dose-dependent reduction of MCF-7 cells 24, 48 and 72 hrs after dsRNA4 treatment compared to dsRNAI- or scrambled dsRNA-treatment. Growth inhibition of SW-480 (C), HeLa S3 (D) and A549 cells (E) over a period of 4 days. (F) Growth of normal mammary epithelial cells (HMEC over a period of 4 days after treatment with either dsRNAI, dsRNA4 or scrambled dsRNA in different concentrations (56 nM-2μM).

A central role for polo-like kinases (PLK) in regulating several stages of mitotic progression has been born out in several species. Overexpression of PLK1 is observed in the majority of hitherto analyzed human tumors. PLK1 overexpression is a negative prognostic factor in patients suffering from non-small cell lung cancer, head and neck tumors, esophageal carcinomas and melanomas. In order to define the role of PLK1 for mitotic progression of human cells and for neoplastic cell growth, phosphorothioate antisense oligonucleotides (ASOs) were tested to selectively downregulate PLK1 expression in MDA-MB-435 (breast cancer), HeLa S3 (cervical carcinoma) and A549 (non-small cell lung cancer) cells. ASOs were identified which suppress PLK1 mRNA and protein in a dose-dependent and sequence-specific manner. This approach also led to reduced PLK1

serine/threonine kinase activity. Downregulation of cellular PLK1 levels in cancer cells altered cell cycle progression moderately with an elevated percentage (20-30%) of cells in G_2/M. Furthermore, cells with reduced PLK1 protein gained a rounded phenotype with multiple centrosomes. Moreover, ASO treatment resulted in potent antiproliferative effects in cell culture. Considerable antitumor activity was observed in vivo against A549 cells. This study suggests that antisense inhibitors targeted against PLK1 at well tolerated doses may be considered as a cancer therapeutic agent.

The mammalian polo-like kinase (PLK1) is structurally related to the polo gene product of Drosophila melanogaster, Cdc5p of Saccharomyces cerevisiae and plo1$^+$ of Schizosaccharomyces pombe. This emerging family of serine/threonine kinases is highly conserved from yeasts to humans. The ability to regulate multiple stages of the mitotic progression is the hallmark of polo-like kinases (plks). Detailed information about the role of plks for mitotic progression came from genetic studies on Drosophila polo, the founding member of the family. Drosophila mutants homozygous for a strong mutant polo allele die as larvae (Llamazares et al., 1991; Sunkel et al., 1988). Flies with a weaker mutant allele produce embryos with severe mitotic defects such as condensed chromosomes with irregular microtubule arrays and a lack of organized centrosomes. Additional genetic approaches provided further insight into the function of the putative yeast homologues of polo. In Saccharomyces cerevisiae mutations in the CDC5 gene cause abnormalities in both mitotic and meiotic divisions (Byers et al., 1974; Hartwell et al., 1973; Sharon et al., 1990). CDC5 mutants arrest in late mitosis as large, budded cells with partially segregated nuclei on an elongated spindle (Kitada et al., 1993). Furthermore, loss of plo1$^+$ function in Schizosaccharomyces pombe has two consequences: It leads to either a mitotic arrest in which condensed chromosomes are associated with a monopolar spindle or following the completion of nuclear division to a failure in septation (Ohkura et al., 1995). Taken together, deletion or strong mutations in plk-coding genes of different species cause severe

growth retardation or even cellular lethality suggesting that plks play key roles for the mitotic progression of lower eukaryotes.

Whereas the yeasts can achieve cell-cycle progression utilizing a single cyclin-dependent kinase, mammals have evolved multiple forms of both Cdks and their activating Cdc25 phosphatases. The phylogenetic development of the plk family is comparable. In contrast to lower eukaryotes, which possess only one plk gene, at least three PLKs (PLK1, PLK21,5NK, PLK31FNK) could be isolated from mammalian cells (Clay et al., 1993; Golsteyn et al., 1994; Holtrich et al., 1994; Holtrich et al., 2000; Lake et al., 1993; Li et al., 1996; Simmons et al., 1992). Their specific functions are very complex and in particular their ability to complement each other remains to be elucidated. We identified human PLK1 and could demonstrate that levels of PLK1 transcripts and protein are elevated in tissues and cells exhibiting a high mitotic index including tumors and immortalized cell lines (Clay et al., 1993; Golsteyn et al., 1994; Holtrich et al., 1994; Lake et al., 1993; Yuan et al., 1997). An increasing body of evidence suggests that the frequency of PLK1 expression is of prognostic value for patients suffering from different types of tumors like non-small cell lung cancer, squamous cell carcinomas of head and neck, melanomas and esophageal carcinomas (Knecht et al., 1999; Strebhardt et al., 2000; Tokumitsu et al., 1999; Wolf et al., 1997). The importance of PLK1 as measure for the aggressiveness of a tumor and its key role for cellular proliferation raise the question whether the inhibition of the PLK1 function in mammalian cells induces as dramatic effects as previously observed in lower eukaryotic cells.

Increasing knowledge about the genetic control of cellular proliferation provides the basis for the rational design of specific therapeutic strategies aimed at the regulation of proliferative disorders such as cancer. Although certain unanswered questions concerning the applicability of the antisense technology remain (Stein, 1995; Wagner, 1995), this experimental

approach can, when targeted to key elements of proliferation-relevant signaltransduction pathways, prevent the development of specific human cancers. Several phosphorothioate antisense oligonucleotides (ASOs) are currently being evaluated in patients suffering from different types of cancer such as ovarian, colon, lymphoma and melanomas (Crooke, 2000).

Furthermore, studies in which these drugs are used in combination with traditional chemotherapeutic agents are in progress.

To elucidate the role of PLK1 for the inhibition of tumor cell growth, in the present study we tested the potential of phosphorothioate ASOs targeted against human PLK1 to inhibit its mRNA and protein expression. We then evaluated the effects of PLK1-specific ASOs on the proliferative activity of human tumor cells (breast cancer, MDA-MB-435; non-small cell lung cancer, A549 and cervical carcinoma, HeLa S3) in vitro and in vivo to shed light on the role of PLK1 as target for cancer treatment.

The work leading to the present invention therefore also provides for phosphorothioate ASOs targeted agains PLK1 and their use for treatment of proliferative diseases like for example cancer diseases. Such phosphorothioate AOS are further subject matters of the present invention as well as their uses.

ASOs inhibit specifically the expression of PLK1 mRNA and protein

26 phosphorothioate ASOs, each 20 nucleotides in length and predicted to hybridize with human PLK1 mRNA were tested to identify effective candidates capable of inhibiting PLK1 gene expression in human tumor cells. These ASOs were homologues to different regions of PLK1 mRNA, with 9 ASOs targeted to the 5'-untranslated region, 6 targeted to sites within the coding region of PLK1 and 11 targeted to the 3'-untranslated region (Fig. 6 a). Binding of ASOs to the complementary sequence of the

mRNA for a specific gene results in gradual downregulation of the protein and loss of function of that gene mostly due to the activation of RNase H, which cleaves the mRNA at RNA/DNA duplex sites (Dirksen et al., 1981). Since phosphorothioates are excellent substrates for RNase H, antisense activity for each of these ASOs was evaluated with Northern blot analyses using a PLK1-specific probe.

Treatment of MDA-MB-435 breast cancer cells in vitro with ASOs against PLK1 at a concentration of 250 nM in the presence of uptake-enhancing cationic lipids (DOTAP) led in few cases to an essential loss of PLK1 mRNA within 24 hrs as demonstrated in figure 6b. The evaluation of Northern blots standardized to the expression of actin or glyceraldehyde-3phosphate dehydrogenase (G3PDH) mRNA revealed that the ASOs, named P12 and P13, which target the 3'-untranslated domain, are efficient inhibitors for reducing PLK1 mRNA in cultured human MDA-MB-435 cells to levels of 30% and 40%, respectively compared to DOTAP-treated cells. Still, most tested ASOs had limited or no influence on the level of endogenous PLK1 mRNA. Furthermore, two control ASOs (HSV-ASO derived from Herpes Simplex Virus and a nonsense-ASO representing a random sequence) led only to a weak reduction. Specific reduction by the ASOs P 12 and P 13 could not only be demonstrated for MDA-MB-435 cells but also for other tumor cell types like HeLa S3 and A549 (Fig. 6 c, d).

To determine whether decreases in PLK1 mRNA levels induced by ASOs were accompanied by corresponding reduction in protein levels, Western blot analyses were performed to evaluate the expression in different tumor cell lines after single application of ASOs. Significant inhibition ($p < 0.001$) of the 68 kDa-PLK1 protein in MDA-MB-435 cells was observed with the ASOs P12 (80%) and P13 (73%) which were previously shown to be potent inhibitors of gene expression (Fig. 7a). A reduction of PLK1 mRNA induced by the application of P12 and P13 resulted also in a significantly lower level ($p < 0.05$) of the corresponding protein in HeLa S3 (P12: 87%;

P13: 47%) and A549 cells (P12: 74%; P13: 61 %) (Fig. 7b, c).

Specificity of the ASO action requires that the outcome is dose-dependent and proportional to the downregulation of the gene. To test for specificity, the concentration of P12 and a control ASO (HSV) was correlated to protein levels of PLK1. The treatment of HeLa S3 and MDAMB-435 cells with P12 exhibited a dose-dependent reduction of PLK1 expression with a median inhibitory concentration (IC50) of 50-75 nM (Fig. 2d, e). The control ASO (HSV) had no significant effect in Western blot analyses. The expression of other cellular proteins such as actin and p38 (MAP kinase family) was not influenced significantly indicating that the effects on cells treated with P 12 are sequence-specific for PLK1.

To directly assess whether downregulation of PLK1 protein level correlates also to reduced PLK1 kinase activity, immunoprecipitated PLK1 from HeLa S3 cells was subjected to enzymatic tests. Figure 2f shows the kinase activity of PLK1 precipitated with immune sera from P12-, control ASO (HSV)- and untreated cells. Although approximately equal amounts of PLK1 protein were present in the three immunoprecipitates, in P12-treated cells phosphorylation of exogenous casein was reduced to 50% of the enzymatic level in control cells. Virtually no kinase activity was detected in the preimmune precipitate (data not shown). These results suggest that the amount of PLK1 protein was specifically reduced in P12-treated cancer cells correlating with low levels of PLK1 activity.

PLK1-specific ASOs inhibit the growth of cancer cells in vitro

It was of particular interest to determine whether ASOs which reduce PLK1 expression influence the proliferation rate of tumor cells. For this purpose MDA-MB-435 cells were treated once with either P12, P13 or a control ASO (HSV) at a concentration of 250 nM. The growth rate of $5x10^5$ cells was determined over a period of 2 days. The treatment with the lipofection

agent (DOTAP) alone or a control ASO (HSV) had only limited effect on the growth rate of MDA-MB-435 cells. In contrast, P12 and P13 had a significant antiproliferative effect ($p<0.05$) of approximately 98% and 93% compared to DOTAP-treated MDA-MB-435 cells within 48 hrs (Fig. 8a). In addition, the remaining 24 ASOs, which had been tested for their ability to reduce the endogenous level of PLK1 mRNA, were utilized to measure their potential to influence the growth of MDA-MB-435. The analysis revealed that those ASOs, which induced only a slight reduction of cellular mRNA, had only limited inhibitory effect on the proliferation of the breast cancer cell line MDA-MB-435 (data not shown). Whether the reduction of proliferative activity is cell type-specific or can also be achieved in other cancer cell lines was subsequently examined. P12 and P13 were shown to determine the extent of growth inhibition also significantly in HeLa S3 cells ($p<0.001$) and in A549 cells ($p<0.05$) suggesting that PLK1 expression is essential for the proliferation of different types of cancer cells (Fig. 8 b, c). Additional evidence for the specific activity of the inhibitory ASO P12 came from a dose-dependent reduction of cell growth in MDA-MB-435 and in HeLa S3 cells (Fig. 8d, e). Increasing concentrations of P12 (50-250 nM) reduced the number of MDA-MB-435 cells by 80% and the number of HeLa S3 cells by 95% within 24 hrs compared to control cells. While maximal protein reduction was achieved in HeLa S3 cells with 100 nM (Fig. 7d), a concentration of 250 nM was required for MDA-MB-435 cells. In both cell lines 250 nM were necessary for maximal growth inhibition.

Reduced levels of PLK1 protein induce mitotic abnormalities

To determine whether the death of ASO treated cells was associated with cell cycle arrest or phenotypic abnormalities, we used FACS-analysis and laser scanning microscopy. Flow cytometric analyses of all three cell lines demonstrated that the induction of the G_2/M cell cycle arrest was moderate. The ASO treatment resulted in an increase of cells in G2/M Of

approximately 20-30% (data not shown).

Previous observations have demonstrated that microinjection of PLK1-specific antibodiesresulted in abnormal distribution of condensed chromatin and monoastral microtubule arrays that were nucleated from duplicated but unseparated chromosomes (Lane et al., 1996). Here we showed for the first time the reduction of endogenous PLK1 protein and corresponding PLK1-kinase activity in cancer cells. To analyze cell cycle phenotypes of P12-treated cells under these conditions, we immunolabeled A549 cells. Antibodies directed against α-tubulin to visualize the spindle apparatus and γ-tubulin to localize centrosomes were used 48 hrs after transfection with P12 and HSV-ASO, respectively. While most of the HSV-ASO-treated cells proceeded through mitosis without abnormal phenotypes, many cells incubated with P12 gained a rounded shape and lost adherence to the cell culture plastic. Whereas application of HSV-ASOs preserved normal centrosome maturation in A549 lung cancer cells, P12-treated cells displayed often unseparated chromosomes and multiple centrosornes (Fig. 9). Partially separated chromosomes induced the formation of nuclear membranes enclosing at least one centrosome. This led to abnormal distribution of centrosomes in interphase cells as demonstrated in figure 9 (a, b).

In vivo antitumor activity of PLK1 ASOs

Having demonstrated that PLK1 ASOs are capable of inhibiting growth of cancer cells in culture in a target- and sequence-specific manner, we tested whether P12 and P13 have also an inhibitory capability in vivo. For this purpose tumor fragments derived from a serial passage of three consecutive transplantations of A549 cells were implanted subcutaneously in nude mice. Xenograft mice bearing a tumor of 100 mm^3 in volume were treated with 12 mg/kg by bolus intravenous injection once daily. The influence of P12 and P13 on the growth of A549 tumors was examined

and compared to effects exerted by a control ASO (HSV) or PBS alone. The administration of both ASOs P12 and P13 at a dose of 12 mg/kg over a period of 24 days revealed a significant effect on the growth of A549 tumors in mice (Fig. 10a). PLK1 ASOs administered systematically inhibited the growth of A549 tumor xenografts in nude mice by 70% (P12) and 86% (P13), respectively. In contrast, no influence was observed when the tumor-bearing animals were treated with a control ASO (HSV) or PBS alone. The efficacy of ASO treatment on the inhibition of PLK1 expression in tumor cells was confirmed by an immunohistochemical analysis: While administration of control ASOs (12 mg HSV/kg) for a period of 24 days had no significant effect on the frequency of PLK1-positive cells (76%), marked reduction of PLK1-positive cells (10%) was observed in P12- and P13-treated animals (Fig. 10b). Staining with the conventional marker for cellular proliferation MIB-I revealed a reduction from 61% to 8% of immunostained proliferating cells in tumors.

Different experimental approaches had the goal to define the function of PLK1 in mammalian cells by altering the level of PLK1 expression. First, the inhibition of PLK1 function through antibody microinjection blocked centrosome maturation in both nonimmortalized human Hs68 fibroblasts and HeLa cervical carcinoma cells (Lane et al., 1996). While PLK1-injected HeLa cells revealed severe mitotic defects such as immature centrosomes, nonimmortalized human Hs68 fibroblasts arrested in G_2 suggesting a centrosome-maturation checkpoint sensitive to alterations in PLK1 function. Second, results from transient expression of dominant negative PLK1 differed from previous antibody microinjection experiments in that most of the mitotic HeLa cells were bipolar and cytokinesis seemed to be disrupted (Mundt et al., 1997). Third, adenovirus delivery of a don-finant-negative PLK1 induced apoptosis in different tumor cell lines (Cogswell et al., 2000). In contrast, normal human mammary epithelial cells arrested in mitosis, but seemed to escape the loss of centrosome maturation and mitotic defects observed in different cancer cells. Thus, the

use of different methods to abrogate the activity of PLK1 revealed its essential role for mitotic progression in mammalian cells. Interestingly, recent data extend previous observations by further showing that the majority of tested tumor lines are more sensitive to the inhibition of PLK1 function than normal epithelial cells (Cogswell et al., 2000). These results suggest that certain tumors show a selective apoptotic response versus normal epithelial counterparts. Still, the methods used in different studies are not suited for the systemic treatment of tumor-bearing animals or cancer patients. Antisense-based methods, which have been proven to inhibit the expression of certain critical cancer genes specifically, have already entered different clinical studies (Agrawal, 1996; Crooke et al., 1994; Zhang et al., 1995). The antisense drug Vitravene has now been approved for the treatment of patients with cytomegalovirus- induced retinitis (Crooke, 1998). Thus, we pursued the goal to test PLK1 as a possible target for cancer therapeutic intervention using an antisense oligonucleotide-based approach by reducing the endogenous level of PLK1 specifically in vitro and in vivo.

In contrast to many chemotherapeutical agents for the treatment of cancer cells, ASOs have the intriguing advantage to act specifically on the gene of interest. To test the specificity of our approach in detail, we analyzed the potential of different PLK1 ASOs to reduce the intracellular level of PLK1 expression and to act in an antiproliferative manner. As expected only very few ASOs were able to reduce the intracellular mRNA level, because due to the three-dimensional structure of mRNA only certain sequence domains are accessible for the heteroduplex formation with ASOs. Two ASOs P12 and P13 targeted against the 3'-untranslated region of human PLK1 mRNA were shown to be potent inhibitors of PLK1 mRNA and protein expression in cell culture. These ASOs displayed IC50 values of 50 nM. Interestingly, our experiments revealed an antisense response, which seemed to reflect the level of endogenous transcripts in the cancer cells examined: For example, the A549 cells with the highest frequency of expression showed

only a moderate response. Still, we can not rule out a homeostatic regulation, which can answer a decrease in mRNA concentration with a metabolic compensation. Administration of P12 and P13 to A549-tumor-bearing mice resulted in reduced PLK1 expression and in potent antiproliferative effects.

ASOs represent a potentially powerful method of selectively inhibiting gene expression. However, the study of antisense compounds has been hampered by some parameters resulting in variable experimental results. ASOs and in particular phosphorothioate versions used in many investigations are highly charged macromolecules that can induce toxic effects or might alter cellular functions via association to endogenous proteins which activate non-antisense mechanisms (Kuss et al., 1999). Biological activity attributed to such ASOs may not be the result of the specific inhibition of a target gene. Thus, demonstration of specificity is a key aspect for concluding true antisense action underlying the biological impact of a specific ASO. For this reason we paid considerable attention to the specificity of inhibition of PLK1 gene expression. Several experiments provided evidence for a specific mode of action by ASOs P12 and P13: (i) During an examination of 26 phosphorothioate ASOs targeted to different sites within the PLK1 mRNA, only a few candidates were potent inhibitors of PLK1 expression. (ii) Control ASOs (HSV-derived, nonsense) had no significant effect on PLK1 mRNA and protein expression in cell culture and in Xenograft experiments. (iii) Our data revealed that the suppression of PLK1 by ASOs was dose-dependent. In addition, we could demonstrate that the expression of other cellular genes like actin and p38 was not affected by P12 or P13 treatment.

The number of antisense cancer drugs that have entered clinical trials is increasing. At least four of these compounds are currently in phase 11 trials including those targeting protein kinase Galpha, bcl-2, c-raf and H-ras (Cunningham et al., 2000; Nemunaitis et al., 1999; O'Dwyer et al., 1999;

Waters et al., 2000; Yuen et al., 1999). Various studies suggest that the inhibition of early steps in signaltransduction causes the simultaneous activation of alternative, parallel signaling pathways resulting also in cellular proliferation. Thus, ASOs targeted against c-raf kinase led only to a transient inhibition of cellular growth (Monia et al., 1996). This effect might be due to the turnover of applied ASOs or due to the location of the raf protein in the signaling cascade. In contrast to early steps in signaltransduction represented by c-raf, ras, PKC, which are targets of antisense approaches, PLK1 is the first example of a kinase triggering terminal steps in the signaling cascade. Multiple observations provided evidence for a central role of PLK1 in the mitotic progression in mammalian cells which can not be by-passed on alternative routes of signal transduction (Cogswell et al., 2000; Lane et al., 1996; Mundt et al., 1997). Moreover, inhibition of PLK1-function was shown to induce tumor-selective apoptosis compared to normal epithelial cells. Considering these observations our experimental data suggest PLK1 as new target for cancer treatment. In addition to phosphorothioate ASOs, modified derivatives with altered sugar moiety or backbone which have improved pharmacokinetical and toxicological properties or low molecular weight inhibitors targeted against human PLK1 need to be developed for future therapeutic endeavors.

Oligonucleotides and antibodies

Phosphorothioate oligonucleotides (ASOs) were synthesized and purified by MWG Biotech (Ebersberg). Monoclonal PLK1-antibodies were obtained from Transduction Laboratories (Heidelberg) for Western blots and from Zytomed (San Francisco, USA) for kinase assays. Antibodies for actin were purchased from Sigma (Deisenhofen) and for p38 from Santa Cruz.

RNA preparation

For isolation of total RNA an RNA-easy-kit was used according to the manufacturer's protocol (Qiagen, Hilden). At least $5x10^5$ cells were used for preparation of total RNA.

Northern blot hybridization

Radiolabeling of the antisense strands of PLK1, ß-actin and G3PDH was performed using 250 μCi of [α-P^{32}]dCTP (6000 Ci/mmol; 1Ci ≙ 37 GBq) for each reaction, 50 μM of each other dNTP and 10 pmol (each) of primer PLK1-17-low (5'-tgatgttggcacccttcagc-3'), actin-2-low (5'-catgaggtagtcagtcaggtc-3') and G3PDH-2 (5'-tccctgcctctactggcgct-3') as described previously (Hock et al., 1998). Northern blotting and hybridizations were carried out as described (Wolf et al., 1997).

Cell Culture

DMEM and DMEM/F-12 1:1 mixture were obtained from Sigma, Ham's F12 and FCS from PAA. PBS, OPTIMEM, glutamine, penicillin /streptomycin and trypsin were purchased from Invitrogen. Tumor cell lines MDA-MB-435 and A549 were obtained from CLS (Heidelberg), HeLa S3 from DSMZ (Braunschweig) and cultured according to their instructions with slight modifications.

Western Blot Analysis

48 hrs after ASO treatment cells were lysed for subsequent Western blotting (Hock et al., 1998). Membranes were kept for 1 hr with monoclonal PLK1 antibodies (1:250) and monoclonal actin antibodies (1:200.000) followed by incubation with goat anti-mouse antibodies (1:2.000) for 30 min. Western blots were performed as described (Bohme

et al., 1996).

Kinase Assays

Cells were lysed 24 hrs after ASO treatment for determination of PLK1 kinase activity. Endogenous PLK1 was immunoprecipitated using monoclonal PLK1 antibodies (Zytomed) and then incubated with 0.5-1 μg of substrate and 2 MCi of [γ^{32}-P]ATP for 30 min at 37°C in kinase buffer (20 mM HEPES pH 7.4,150 mM KCl, 10 MM $MgCl_2$, 1 mM EGTA, 0.5 mM DTT, 5 mM NaF, 0.1 mM Na_3V0_4). Kinase reaction was stopped and fractionated on a 12% SDS-polyacrylamide gel (BioRad, München).

Indirect Immunofluorescence

Cells were stained as described before (Holtrich et al., 2000). Antibodies were used as follows: monoclonal α-tubulin (Cedarlane, Canada) 1: 100, polyclonal rabbit PLK1 (Yuan et al., 1997) 1: 100 or monoclonal γ-tubulin (Sigma) 1: 100.

In vitro application of ASOs and determination of cell proliferation.

In vitro-inhibitory activities of ASOs on cell proliferation were tested by transfection with different ASOs. Transfections were performed using the DOTAP method (Roche, Mannheim). In brief, I day before transfection cells were split to a density of $5x10^5/25cm^2$-culture flask corresponding to a density of 40-50% at the time of transfection. Cells were treated with ASOs at a concentration of 250 nM. After 3,5 hrs incubation with ASOs in OPTIMEM with DOTAP at 37°C, transfection mix was replaced by normal culture media. Cell numbers were determined at the appropriate time after ASO treatment by direct counting using a hemacytometer. Cell viability was assessed by trypan blue staining. Each experiment was performed at least in triplicate and the standard deviation for each group was

determined.

Tumor xenograft studies

Human cancer xenograft models were established with at least 3 independent groups of 5 athymic nude mice (nu/nu) NMRI 8-10 weeks old (Harlan Winkelmann). For this purpose A549 cells were harvested, washed with PBS, resuspended in normal culture media and then $2x10^6$ cells were injected subcutanously into the animals flank regions. Arising tumors were serially passaged by a minimum of three consecutive transplantations before the start of treatment. Then tumor fragments were implanted subcutaneously in both flanks of the nude mice and ASO application was started 25 days after transplantation when the tumor reached a volume of 100 mm^3. ASO treatment (formulated in PBS) was carried out daily by bolus injection (100 μl) into the animals tail vein at a dose of 12 mg/kg body mass for 24 days. Tumor diameters were determined using a caliper. Volumes were calculated according to the formula $V = 7t/6$ x largest diameter x smallest diameter. Standard deviations were calculated. Experiments were carried out in triplicate. After sacrificing the animals tumors were excised for immunohistochernistry (Yuan et al., 1997).

Immunohistochemistry

Tumor sections of Xenograft tumors were prepared as described (Yuan et al., 1997). Slides were incubated with monoclonal MIB-I antibodies (1:10; Dianova, Hamburg) and a polyclonal PLK1 antibody (1:200; Transduction Laboratories, Heidelberg). As detection system for PLK1 the EnVision+System (Dako, Hamburg) was used according to the manufacturer's protocol.

Quantitative analysis

For semiquantitative analysis of Northern and Western blot signal intensities the autoradiographs were scanned using a Kodak gel documentation system (ID 3.5). After integration of signal intensities expression of PLK1 and actin were correlated for quantitative comparison. The expression values were given in percentage of control. For quantitative evaluation of immunohistochernistry in A549 tumors, 10 high power magnification fields (400x) per slide were analyzed. Immunoreactive staining of PLK1 and MIB-I is given in percent positive tumor cells.

Figure legends

Fig. 6. Reduction of PLK1 mRNA in vitro. (a) Relative positioning of the predicted hybridization sites of the 26 tested PLK1 ASOs. Sequences of all ASOs are available upon request. Arrows indicate positions of the potent ASOs P12 and P13. (b) Northern blot analysis of PLK1 mRNA in MDA-MB-435 cells 24 hrs after ASO treatment. HSV-ASO served as negative control. To ascertain uniformity of loading the membrane was reprobed with human B-actin and G3PDH. Percent inhibition was calculated by comparison with standardized PLK1 mRNA levels of cells grown in the absence of ASOs. PLK1 mRNA expression in HeLa S3 cells (c) and A549 cells (d) 24 hrs after ASO application. Membranes were reprobed with human 13-actin.

Fig. 7. Inhibition of PLK1 protein expression and kinase activity by PLK1-specific, ASOs in cancer cells. Control cells were incubated with OPTIMEM. HSV-ASO served as negative control. Percent inhibition was calculated by comparison with PLK1 protein levels in cells grown in the absence of ASOs. (a) Western blot analysis of PLK1 protein in MDA-MB-435 cells 48 hrs after ASO treatment. Indicated are the signals for PLK1 and actin in both autoradiographs. Actin served as control for equal loading (upper panel). Quantification of PLK1 protein levels after normalization to actin was performed using a Kodak gel documentation system (ID 3.5). Mean values of at least 3 independent experiments with standard deviation are shown (lower panel). Quantification of PLK1 protein in HeLa S3 cells (b) and A549 cells (e) after normalization to actin. PLK1 protein correlated to the concentration of ASO P12 in HeLa S3 cells (d) and in MDA-MB-435 cells (e). PLK1 immunoprecipitated from ASO treated cells phosphorylated casein to a lower extent compared to PLK1 from control cells (upper panel). Coomassie staining served as control for equal loading of substrate (middle panel) Equal amounts of PLK1 were subjected to the

enzymatic assay (lower panel) (f).

Fig. 8. Antiproliferative effects of PLK1 antisense inhibition in cancer cells. Control cells were incubated only with OPTIMEM. HSV-ASO served as a control. Percent inhibition was calculated by comparison to the number of cells treated with DOTAP grown in the absence of ASOs. (a) Growth inhibition of MDA-MB-435 cells treated with ASOs at a concentration of 250 nM over a period of 2 days. Growth inhibition of HeLa S3 (b) and A549 cells (c) over a period of 3 days. Dose-dependent reduction of MDA-MB-435 cells (d) and HeLa S3 cells (e) after ASO treatment. Mean values of at least 3 independent experiments with standard deviation are shown.

Fig. 9. ASO treatment induced abnormal centrosome distribution in A549 cells. Cells were transfected with PLK1 ASOs and immunostained 48 hrs post transfection for y-tubulin. Interphase cells displayed abnormal localization of multiple centrosomes. Laserscan images (a and b) represent characteristic interphase figures.

Fig. 10. Effects of PLK1 ASOs on the growth of A549 tumors in nude mice. (a) Growth inhibition of two PLK1 ASOs (P12, P13) in contrast to control ASO (HSV)-treated and to untreated control mice. ASO administration was initiated 25 days after transplantation and continued for 24 days. Mean values of at least 3 independent experiments with standard deviation are shown (*: $p<0.05$). (b) Immunohistochernical analysis of PLK1 and MIB-I in A549 tumor xenografts after treatment. A, PLK1 expression in ASO (I-ISV)-treated animals. PLK1 expression in P12-treated animals. C, MIBA expression in ASO (HSV)-treated animals. D, MIB- I expression in P12-treated animals.

References

Agrawal S. (1996). Trends Biotechnol., 14, 376-387.

Bohme B, VandenBos T, Cerretti DP, Park LS, Holtrich U, Rübsamen-Waigmann H, and Strebhardt K. (1996). J Biol. Chem., 271 , 24747-24752.

Byers B and Goetsch L. (1974). Cold Spring Harb. Symp. Quant. Biol., 38, 123-131.

Clay FJ, McEwen SJ, Bertoncello I, Wilks AF, and Dunn AR. (1993). Proc.Natl.Acad.Sci. US.A, 90, 4882-4886.

Cogswell JP, Brown CE, Bisi JE, and Neill SD. (2000). Cell Growth Differ., 11, 615-623.

Crooke ST. (1998). Antisense Nucleic Acid Drug Dev., 8, vii-viii.

Crooke ST. (2000). Oncogene, 19 , 6651-6659.

Crooke ST, Grillone LR, Tendolkar A, Garrett A, Fratkin MJ, Leeds J, and Barr WH. (1994). Clin. Pharmacol. Ther., 56, 641-646.

Cunningham CC, HoWund JT, Schiller JH, Geary RS, Kwoh TJ, Dorr A, and Nemunaitis J. (2000). Clin. Cancer Res., 6, 1626-1631.

Dirksen ML and Crouch RJ. (1981). J Biol. Chem., 256, 11569-11573.

Golsteyn RM, Schultz SJ, Bartek J, Ziemiecki A, Ried T, and Nigg EA. (1994). J. Cell Sci., 107 (Pt 6), 1509-1517.

Hartwell LH, Mortimer RK, Culotti J, and Culotti M. (1973). Genetics, 74, 267-286.

Hock B, Bohme B, Kam T, Yamamoto T, Kaibuchi K, Holtrich U, Holland S, Pawson T, Rübsamen-Waigmann H, and Strebhardt K. (1998). Proc.Natl AcadSci. U.S.A, 95, 9779-9784.

Holtrich U, Wolf G, Brauninger A, Kam T, Bohme B, Rübsamen-Waigmann H, and Strebhardt K. (1994). Proc.Natl.Acad.Sci. U.S.A, 91, 1736-1740.

Holtrich U, Wolf G, Yuan J, Bereiter-Hahn J, Kam T, Weiler M, Kausetmann G, Rehli M, Andreesen R, Kauftnann M, Kuhl D, and Strebhardt K. (2000). Oncogene, 19, 4832-4839.

Kitada K, Johnson AL, Johnston LH, and Sugino A. (1993). Mol. Cell Biol., 13, 4445-4457.

Knecht R, Elez R, Oechler M, Solbach C, von Ilberg C, and Strebhardt K. (1999). Cancer Res., 59 , 2794-2797.

Kuss B and Cotter F. (1999). Ann. Oncol., 10, 495-503.

Lake RJ and Jelinek WR. (1993). Mol. Cell Biol., 13, 7793-7801.

Lane HA and Nigg EA. (1996). J Cell Biol., 135, 1701-1713.

Li B, Ouyang B, Pan H, Reissmann PT, Slamon DJ, Arceci R, Lu L, and Dai W. (1996).J.Biol. Chem., 271, 19402-19408.

Llamazares S, Moreira A, Tavares A, Girdharn C, Spruce BA, Gonzalez C, Karess RE, Glover DM, and Sunkel CE. (1991). Genes Dev., 5, 2153-2165.

Monia BP, Sasmor H, Johnston JF, Freier SM, Lesnik EA, Muller M, Geiger T, Altmann KH, Moser H, and Fabbro D. (1996). Proc.Alatl AcadSci. U.S.A, 93, 15481-15484.

Mundt KE, Golsteyn RM, Lane HA, and Nigg EA. (1997). Biochem. Biophys. Res. Commun., 239 , 377-385.

Nemunaitis J, Holmlund JT, Kraynak M, Richards D, Bruce J, Ognoskie N, Kwoh TJ, Geary R, Dorr A, Von Hoff D, and Eckhardt SG. (1999). J Clin. Oncol., 17, 3586-3595.

O'Dwyer PJ, Stevenson JP, Gallagher M, Cassella A, Vasilevskaya 1, Monia BP, Holn-Aund J, Dorr FA, and Yao KS. (1999). Clin. Cancer Res., 5, 3977-3982.

Ohkura H, Hagan IM, and Glover DM. (1995). Genes Dev., 9, 1059-1073. Sharon G and Simchen G. (1990). Genetics, 125, 475-485.

Simmons DL, Neel BG, Stevens R, Evett G, and Erikson RL. (1992). Mol. Cell Biol., 12, 4164-4169.

Stein CA. (1995). Nat. Med, 1, 1119-1121.

Strebhardt K, Kneisel L, Linhart C, Bernd A, and Kaufmann R. (2000). JAMA, 283, 479-480.

Sunkel CE and Glover DM. (1988). J. Cell Sci., 89 (Pt 1), 25-38.

Tokumitsu Y, Mori M, Tanaka S, Akazawa K, Nakano S, and Niho Y. (1999). Int. J Oncol., 15, 687-692.

Wagner RW. (1995). Nat. Med, 1, 1116-1118.

Waters JS, Webb A, Cunningham D, Clarke PA, Raynaud F, di Stefano F, and Cotter FE. (2000). J Clin. Oncol., 18, 1812-1823.

Wolf G, Elez R, Doermer A, Holtrich U, Ackermann H, Stutte HJ, Altmannsberger HM, Rübsamen-Waigmann H, and Strebhardt K. (1997). Oncogene, 14, 543-549.

Yuan J, Horlin A, Hock B, Stutte HJ, Rubsamen-Waigmann H, and Strebhardt K. (1997). Am.JPathoL, 150, 1165-1172.

Yuen AR, Halsey J, Fisher GA, Holrnlund JT, Geary RS, Kwoh TJ, Dorr A, and Sikic BI. (1999). Clin.Cancer Res., 5 3357-3363.

Zhang R, Yan J, Shahinian H, Amin G, Lu Z, Liu T, Saag MS, Jiang Z, Temsamani J, Martin RR, and. (1995). Clin. Pharmacol. Ther., 58, 44-53.

Polo-like kinases regulate multiple stages in mitosis. Plk1 is overexpressed in tumors. The carboxyterminal regions of Plks contain a conserved region, termed polo-box, which is required for subcellular localization and for physical interaction with substrates. We linked the polo-box (aa 410-429) of Plk1 to an Antennapedia peptide and studied its impact on tumor cells. The polo-box inhibited phosphorylation of substrates by Plk1 in a dose dependent manner. While the wild-type polo-box inhibited the proliferation of tumor cells associated with induction of apoptosis, a mutated derivative was much less effective. The treatment caused mitotic arrest, misaligned chromosomes and multiple centrosomes. Taken together, membrane-permeable polo-box-peptides inhibit cancer cell proliferation efficiently.

Polo-like kinases (Plks) are serine-threonine kinases that are highly conserved during evolution. This family includes mammalian Plk1, Plk2 (Snk) and Plk3 (Fnk/Prk), Xenopus laevis Plx1, Drosophila melanogaster polo, Schizosaccharomyces pombe Plo1 and Saccharomyces cerevisiae Cdc5. Increasing evidence supports the concept that Plks regulate pivotal stages throughout mitosis including its initiation by activating Cdc2 through Cdc25 and direct phosphorylation of cyclin B1 targeting Cdc2/cyclin B1 to the nucleus. Furthermore, Plk1 contributes to centrosome maturation, bipolar spindle formation, DNA damage checkpoint adaptation and activation of Cdc16, Cdc27 as components of the anaphase-promoting complex (APC) for mitotic exit. Finally, Plks are key regulators of cytokinesis (for review see Glover et al. (1998) and Nigg (1998)).

Mammalian Plk1 is overexpressed in rapidly proliferating cells and various human tumors (Yuan et al. (1997)). An increasing body of evidence suggests that the frequency of Plk1 expression is of prognostic value for patients suffering from different types of tumors like non-small cell lung cancer, squamous cell carcinomas of head and neck, melanomas,

oropharyngeal carcinomas, ovarian and endometrial carcinomas (Strebhard (2001)). Many data implicate that Plk1 participates in pathways, which override checkpoint arrests. Plk1 is needed for the Ca^{2+}-induced release of Xenopus egg extracts from the meiotic M phase arrest (Descombes and Nigg (1998)). Cdc5p is clearly required for adaptation to a DNA damage checkpoint in Saccharomyces cerevisiae (Toczyski et al. (1997)). Moreover, expression of active Plk1 can override the G_2 arrest induced by DNA damage in mammalian cells (Smits et al. (1997)). Thus, it is tempting to speculate that Plks may play a role in overriding spindle and/or DNA damage checkpoints. Overexpression of Plk1 might be involved in malignant proliferation. Furthermore, constitutive expression of Plk1 in NIH-3T3 cells causes oncogenic focus formation and induces tumor growth in nude mice suggesting that Plk1 may contribute to cancer progression (Smith et al. (1997)). Disrupting the function of Plks could be an important application for cancer therapy.

From the view of the primary structure, Plks contain a strikingly conserved sequence within their C-terminal domain, termed the polo-box, which is 30 amino acids in length. Without impairing kinase activity, three mutations in the polo-box of Plk1 abolish its ability to functionally complement the defect associated with a Cdc5-1 temperature-sensitive mutation (Lee et al. (1996)). Recent studies revealed that fission yeast Plo1 interacts with the APC through the polo-box and the tetratricopeptide repeat domain of the subunit, Cut23 (May et al. (2002)). A mutation in Cut23, which specifically disrupts the interaction with the polo-box, results in metaphase arrest. Taken together, the data suggest that the polo-box of Plks plays a critical role for the function of Plk1, in particular for its spatial distribution and for the physical interaction with substrates.

Due to the rapid development of technical protein synthesis and the advantage of non-gene interference, the treatment with peptides is becoming a powerful new approach for tumor therapy (Latham (1999)). A

16-mer peptide, derived from the homeodomain of Antennapedia, has been reported to enter cells readily via a non-endocytotic and receptor- and transporter-independent pathway (Derossi et al. (1996)). In this communication we have linked this Antennapedia-peptide to the wild-type polo-box or to a mutated polo-box and analyzed its impact on the proliferation of cancer cells.

Synthesis of peptides. Peptides were synthesized according to Fmoc synthesis protocols with double or triple coupling reactions using TBTU as activator on a Symphony synthesizer (Rainin Instrument Co, Woburn, MA, USA). Purifications were performed by RP-HPLC on a Waters (Milford, MA, USA) Delta-Pak C18 column with a Waters liquid chromatography system. Quality control was performed by analytical RP-HPLC using a Waters Alliance 2690 separation module equipped with a Waters 996 photodiode array detector and by MALDI-TOF mass spectrometry. Peptide sequences:
P1 (polo-box (aa 410-429) linked to a 16-mer carrier from Antennapedia):
H2N-WVSKWVDYSDKYGLGYQLCDRQIKIWFQNRRMKWKK-COOH
P2 (mutated polo-box (aa 410-429) linked to a 16-mer carrier from Antennapedia):
H2N-WVSKFADYSDKYGLGYQACDRQIKIWFQNRRMKWKK-COOH
P3 (16-mer carrier from Antennapedia as a control):
H2N-RQIKIWFQNRRMKWKK-COOH

Cell culture and growth inhibition assays. Cancer cell lines HeLa S3 (cervix), MCF-7 (breast) and Saos-2 (osteosarcoma) were grown at 37°C in 5% CO_2 in Ham's F12, RPMI 1640 and McCoy's 5a medium, respectively containing 10% FBS, 2 mM L-glutamine. To assay for growth inhibition, exponentially growing cells (0.3-2.5 x 10^4) were seeded into 24-well plates. On the following day cells were incubated with peptides at varying concentrations without serum for 3 h followed by addition of complete medium. On day 3, 6 and 8 cells were treated again and harvested on day 3, 6, 8 and 10 to determine cell numbers using a

Hemacytometer. Cell viability was assessed by trypan blue staining. Each experiment was repeated at least three times.

Flow cytometry and indirect immunofluorescence staining. Cell cycle analysis was performed using a Cycle TEST™ PLUS DNA reagent kit (Becton Dickinson) according to the manufacturer's instructions. Briefly, cells were washed with PBS, treated with RNase A and stained with propidium iodide (PI). The analysis was performed using a Becton Dickinson FACScan flow cytometer. Using the MODFIT LT 2.0 software (Verity Software House, Topsham, ME) for each individual sample 30,000 cells were analyzed.

For staining cells were grown in slide flasks and treated with peptides for 24 h. Then, cells were fixed in 4% paraformaldehyde for 30 min, permeabilized in 0.2% Triton X-100 for 20 min and stained with α-tubulin (Serotec/Biozol, Eching) 1:100, polyclonal rabbit Plk1 1:100, or monoclonal γ-tubulin (Sigma) 1:100. Stained cells were analyzed with a confocal laser scan microscope (CLSM) or a fluorescence microscope.

Annexin V apoptosis assay. Cells were seeded into 6-well plates, allowed to attach overnight, and then treated with different peptides at a concentration of 10 μM. Cells were trypsinized after 16 h and incubated with Annexin V according to the manufacturer's recommendations (Mo Bi Tech).

In vitro kinase assays. Plk1 purified from Sf 9 cells was incubated with 0.5-1 μg of Plk1-specific substrates and 2 μCi of [γ-^{32}P] ATP for 20 min at 37°C in kinase buffer (20 mM HEPES pH 7.4, 150 mM KCl, 10 mM $MgCl_2$, 1 mM EGTA, 0.5 mM DTT, 5 mM NaF, 0.1 mM Na_3VO_4 and 100 μM ATP).

The polo-box fused to an Antennapedia carrier translocates to the cytoplasm and nucleus of cancer cells. Plk1 was shown to be of

importance for the G_2/M transition (Glover et al. (1998) and Nigg et al. (1998). The polo-box, a highly conserved domain of Plk1 (aa 410-439), contributes to binding of substrates as well as for its correct subcellular localization (Lee et al. (1999) and May et al. (2002)). We assumed that peptides representing the polo-box might be able to compete with Plk1 for endogenous substrates and docking proteins. Thus, we tested polo-box-specific peptides for their ability to suppress the function of endogenous Plk1. In previous experiments an Antennapedia homeodomain sequence was linked to peptides and allowed the resulting chimerical peptides to be transported across the cell membrane directly from the cell culture medium to both, cytoplasm and nuclear compartment (Derossi et al. (1996)). In our study we linked the Antennapedia homeodomain (16 aa) to the core region of the polo-box derived from Plk1 (aa 410-429) (Fig. 11A) or to a mutated version (Lee et al. (1999)) to find out whether fusion peptides could enter tumor cells from the culture medium. The transport kinetics revealed that FITC-labelled peptides reached the cytoplasm within 15 min and then emerged immediately to the nucleus. After 2 h peptides entered 98-100% of cells in culture. Both fusion peptides (wild-type P1 and mutant P2) were efficiently delivered into the cytoplasm and nucleus of MCF-7 (Fig. 11B: e, f), HeLa S3 cells (Fig. 11B: g, h) and Saos-2 cells (data not shown). Peptides were distributed diffusely in the cytoplasm and accumulated at the nuclear membrane. Elevated concentrations of peptides were detected at nucleoli. The overall distribution and uptake of both peptides (wild-type P1 and mutant P2) in HeLa S3 and MCF-7 cells was similar. 4 h after peptide-treatment morphological changes in MCF-7 and HeLa S3 cells due to toxic effects were not observed (Fig. 11B: a-d). FITC-labeled peptides were still detectable after 24 h (data not shown).

Wild-type polo-box P1 inhibits the proliferation of human MCF-7, Saos-2 and HeLa S3 cells. At first the human breast cancer cell line MCF-7 was tested to assay effects exerted by polo-box-specific peptides on its proliferation. A dose kinetics was established to choose an appropriate

working concentration for the treatment of cells. While the wild-type peptide P1 at concentrations between 0.01 and 0.5 μM did not affect the growth behavior, concentrations above 1 μM started to inhibit the proliferation of MCF-7 cells (Fig. 11C). Inhibition of proliferation occurred in a dose-dependent manner in the range between 1-10 μM of P1. A general toxic effect was observed above 20 μM of peptide P1 (data not shown).

To investigate whether antiproliferative effects exerted by polo-box peptides are restricted to certain cell-types, we tested different human cancer lines: MCF-7 (breast), Saos-2 (osteosarcoma) and HeLa S3 (cervix). As shown in figure 2A-C the wild-type polo-box (P1) exerted an inhibitory effect on cell proliferation which was most prominent in MCF-7 cells. Interestingly, the mutated polo-box (P2), which differed from P1 at three positions, reduced the antiproliferative potency of P1 significantly. While an intermediate effect was seen for Saos-2 cells, little inhibition occurred in HeLa S3 cells. The control 16-mer-carrier P3 alone had eventually no effect at concentrations between 5-10 μM. Thus, the results suggested that the inhibitory effect exerted by polo-box peptides is sequence-specific. In addition, testing of primary epithelial cells (HMEC) revealed that the polo-box P1 inhibited proliferation of HMEC, but to a much lower extent than MCF-7 cells.

Treatment of cancer cells with polo-box-specific peptides induces G_2/M cell cycle arrest. Since the functional down-regulation of Plk1 by microinjection of Plk1-specific antibodies or overexpression of a dominant-negative Plk1 induced G_2/M arrest (Lane et al. (1996) and Cogswell et al. (2000)), we investigated the impact of polo-box-specific peptides on the cell cycle of tumor cells. Figure 12D depicts a representative analysis of HeLa S3 cells at day 6. Incubation with the wild-type polo-box P1 induced an increase of cells in G_2/M by 25-35% compared to control cells. We decided further to determine the subpopulation of mitotic cells by microscopical means. The

percentage of mitotic cells increased 3-4 fold after wild-type polo-box (P1) treatment (14.7%) compared to control cells (3.5%) (Fig. 12E). In contrast, the control peptide P3 had no effect. The mutated polo-box P2 exhibited an intermediate inhibitory potential. These data suggest that polo-box-specific peptides have the ability to induce cell cycle arrest at G_2/M.

Polo-box-specific peptides induce apoptosis in cancer cells. Cells treated with peptides were labeled with annexin V biotin and PI to determine the extent of cellular apoptosis. The treatment with wild-type polo-box P1 induced an elevated percentage of apoptotic cells including early phase apoptosis (annexin V-positive) and late phase apoptosis (annexin V- and PI-positive) compared to the control peptide P3 (Fig. 13A, B). To further confirm the finding, we stained the DNA and analyzed the apoptotic phenotype by fluorescence microscopy. In MCF-7 and HeLa S3 cells the typical apoptotic morphology was observed including condensation and fragmentation of nuclear chromatin, shrinkage of the cytoplasm and loss of membrane asymmetry (Fig. 13C: b, d, e, g, i, j). In contrast, no significant increase of apoptotic cells was found in carrier peptide (P3)-treated cells (Fig. 13C: c, h) and non-treated control cells (Fig. 13C: a, f). In cells incubated with the mutated form P2, there was also increased apoptosis, but less extensive compared to the treatment with wild-type polo-box (data not shown).

Wild-type polo-box induces abnormal mitotic phenotypes with misaligned chromosomes and multiple spindle poles. Polo-box-treated cells were further analyzed using DNA- and α-tubulin-staining to monitor spindle apparatus and chromosomal figures. Many treated cells showed multiple (Fig. 13D: d, f) or monoastral spindle poles (Fig. 13D: e). Furthermore, chromosomes in P1-treated HeLa S3 cells were misaligned, not properly segregated and partially condensed (Fig. 13D: a-c).

The polo-box inhibits the phosphorylation of substrates by Plk1 in vitro. Furthermore, we studied potential mechanisms underlying the inhibitory effect on cell proliferation by the polo-box (P1). For this purpose kinase assays using specific substrates of Plk1 were performed (Fig. 14). Whereas the polo-box P1 and its mutated form P2 decreased the phosphorylation of substrates clearly, the carrier peptide P3 exhibited only at high concentrations of 25-50 μM a weak inhibition of phosphorylation. Within a dose range of 6.25 to 25.0 μM the inhibitory effect of the polo-box P1 differs from that of the mutated form P2: wild-type polo-box induced at least two fold more inhibition than its mutated form. In contrast, the carrier P3 showed no effect at all. Below 1.56 μM, only the wild-type polo-box still exhibited some effect. The data suggest that the inhibitory effect of the polo-box could at least partially be due to a reduction of Plk1-specific phosphorylation.

The Antennapedia homeodomain corresponding to the third helix of the DNA binding domain of a Drosophila transcription factor is internalized into eukaryotic cells by a receptor-independent process (Derossi et al. (1996)). The internalization peptide has been used as vector for small peptides derived from c-myc, p21 and p16 to traverse the cell membrane (Giorello et al. (1998), Fahraeus et al. (1998) and Mutoh et al. (1999)). We linked this carrier to a peptide (P1) representing the polo-box of Plk1 or to the mutated polo-box (P2). Fused peptides entered the cells quickly and efficiently. Both polo-box peptides P1 and P2 were found in the cytoplasm and nucleus of cancer cells. No difference in import efficiency between the wild-type polo-box P1 and its mutated form P2 could be detected in HeLa S3, MCF-7 and Saos-2 cells. Toxic side effects were not observed in cell lines at concentrations between 0.01-10 μM.

Plk1 plays various critical roles in the passage of cells through M phase. It is overexpressed in rapidly proliferating cells and tumors (Yuan et al. (1997) and Strebhard (2001)). Data implicate that Plk1 contributes to

override spindle- and DNA damage-checkpoints (Descombes et al. (1998), Toczyski et al. (1997) and Smits et al. (2000)), which makes Plk1 an attractive target for cancer therapy. Recently, it was reported that overexpression of the C-terminal domain of Plk1 is more efficient in causing mitotic delay or arrest than wild-type or kinase-defective Plk1 (Jang et al. (2002)). This observation is due to the binding of the C-terminus to full-length Plk1 or to the catalytic domain of Plk1, which causes the inhibition of its kinase activity (Jang et al. (2002)). The region within the C-terminal domain mediating this effect is unknown. The polo-box represents a highly conserved sequence within the C-terminal noncatalytic region of the Plk-family and has not been observed in proteins other than Plks yet. The exchange of three amino acids within the polo-box abolished the proper localization of Plk1 and disrupted its kinase function (Lee et al. (1999)). In this communication we demonstrated for the first time that a fusion protein containing the polo-box of Plk1 and a transmembrane carrier from Antennapedia used for the treatment of cancer cells is a novel strategy to inhibit the function of Plk1. We revealed that the polo-box inhibits the proliferation of various cancer cell lines by inducing apoptosis. Strong effects were observed in MCF-7 cells which is possibly connected to the functional integrity of wild-type p53 and Rb, two tumorsuppressor proteins leading to better apoptotic reaction. The inhibitory effect began after 10 h of treatment and reached its apoptotic peak at 24 h. The typical morphology of apoptotic cells was observed in all three cancer lines. As reported for microinjecting of Plk1-antibodies or for expression of a dominant-negative form of Plk1 (Lane et al. (1996), Cogswell et al. (2000)), polo-box peptide induced also mitotic arrest. The FACS-analysis documented an increase of the G_2/M-population and in particular a 3-4 fold increase of mitotic cells in polo-box-treated cells.

In many treated cells chromosomes appeared to be randomly distributed and improperly condensed. Multiple or monoastral spindle poles were observed which is in line with observations in cells transfected with

C-terminal domain of Plk1 (Jang et al. (2002)). In addition, polo-box-treated cells displayed daughter cells still connected by strings of cytoplasm. Since P3-treatment did not induce incomplete separation of arising cells, polo-box-mediated functions seemed also to be involved in cytokinesis (data not shown).

Major abnormalities in cancer cells including the inhibitory effect on proliferation were induced only by the wild-type polo-box, but not by the mutated form P2. Different mechanisms could contribute to the apoptotic impact exerted by polo-box peptides. At first, kinase assays revealed an inhibitory effect on substrate phosphorylation by Plk1: The polo-box peptide could prevent the binding of Plk1 to its substrate thereby acting in a competitive manner. Secondly, recent evidence documents that the C-terminal domain of Plk1 can bind to full-length or the catalytic domain of Plk1 (Jang et al., (2002)). This interaction is interrupted when Thr-210 is substituted with an aspartatic residue. In addition, the function of Plk3 was also shown to depend on its C-terminal domain (Conn et al. (2000)). Still, the region within the C-terminal domains of Plk1 and Plk3 responsible for regulating the kinase activity remains to be elucidated. It is intriguing to consider the polo-box, a domain very well conserved during evolution, as candidate for this regulatory function possibly by binding to a region surrounding Thr-210 in Plk1. This hypothesis gains further support from previous observations which demonstrated that mutations in the polo-box reduce the kinase activity of Plk1 (Lee et al. (1999)). Future investigations are required to study the polo-box as structural component for an intramolecular modulation of the activity of Plks.

Whereas in yeasts and Drosophila only a single Plk has been identified to date, the genome of higher vertebrates encompasses at least three Plks. The remaining two family members, Plk2 (Snk) and Plk3 (Fnk/Prk) belong to the category of immediate-early response genes (Glover et al. (1998) and Nigg et al. (1998)). Functional assays imply that Plk1 and Plk3 are

likely to have both overlapping and unique functions within the cell cycle (Glover et al. (1998)). Plk3 links DNA damage functionally to cell cycle arrest and apoptosis partially via the p53 pathway (Xie et al. (2001)). Overexpression of Plk3 induces incomplete cytokinesis and apoptosis (Conn et al. (2000)). Considering the high homology (74%) of the polo-boxes belonging to Plk1-3, we could not exclude that the polo-box-specific peptide (P1) derived from Plk1 may also inhibit at least partially the function of Plk2 and Plk3, which might contribute to the effects observed in our study. Especially inhibition of Plk3 might be involved in inducing apoptosis and incomplete cytokinesis. Taken together, polo-box-specific peptides inhibit proliferation of tumor cell lines by inducing mitotic arrest and apoptosis. In line with the rapid development of peptide synthesis, polo-box could be a powerful inhibitor for proliferation. Up to date Plk1-function was inhibited by expression of dominant-negative forms or by application of antibodies (Lane et al. (1996) and Cogswell et al. (2000)). Beyond perspectives offered by these techniques the use of fusion peptides such as P1 could open new ways for the systemic treatment of animals with localized tumors or even with disseminated disease. Thus, further studies in tumor-bearing animals will shed light on the potential of polo-box-specific peptides as candidates for tumor therapy.

References

1. Glover, D. M., Hagan, I. M. and Tavares, A. A. Polo-like kinases: a team that plays throughout mitosis. Genes Dev., 12:3777-3787, 1998.

2. Nigg, E. A. Polo-like kinases: positive regulators of cell division from start to finish. Curr. Opin. Cell Biol., 10:776-783, 1998.

3. Yuan, J., Hörlin, A., Hock. B., Stutte, H. J., Rübsamen-Waigmann, H. and Strebhardt, K. Polo-like kinase, a novel marker for cellular proliferation. Am. J. Path., 150:1165-1172, 1997.

4. Strebhardt, K. 2001. PLK (polo-like kinase). In Encyclopedia of Molecular Medicine. T.E.Creighton, editor. Wiley and Sons, Inc., New York, N.Y. 2530-2532.

5. Descombes, P. and Nigg, E. A. The polo-like kinase Plx1 is required for M phase exit and destruction of mitotic regulators in Xenopus egg extracts. EMBO J., 17: 1328-1335, 1998.

6. Toczyski, D. P., Galgoczy, D. J. and Hartwell, L. H. CDC5 and CKII control adaptation to the yeast DNA damage checkpoint. Cell, 90: 1097-2106, 1997.

7. Smits, V. A., Klompmaker, R., Arnaud, L., Rijksen, G., Nigg, E. A. and Medema, R. H. Polo-like kinase-1 is a target of the DNA damage checkpoint. Nat. Cell Biol., 2: 672-676, 2000.

8. Smith, M. R., Wilson, M. L., Hamanaka, R., Chase, D., Kung, H., Longo, D. L. and Ferris, D. K. Malignant transformation of mammalian cells initiated by constitutive expression of the polo-like kinase. Biochem. Biophys. Res. Commun., 234: 397-405, 1997.

9. Lee, K. S., Song, S. and Erikson, R. L. The polo-box-dependent induction of ectopic septal structures by mammalian polo kinase, Plk, in Saccharomyces cerevisiae. Proc. Natl. Acad. Sci., USA, 96:14360-14365, 1999.

10. May, K. M., Reynolds, N., Cullen, C. F., Yanagida, M. and Ohkura, H. Polo boxes and Cut23 (Apc8) mediate an interaction between polo kinase and the anaphase-promoting complex for fission yeast mitosis. J. Cell Biol., 156: 23-28, 2002.

11. Latham, P. W. Therapeutic peptides revisited. Nat. Biotech., 17: 755-757, 1999.

12. Derossi, D., Calvet, S., Trembleau, A., Brunissen, A., Chassaing, G. and Porchiantz, A. Cell internalization of the third helix of the Antennapedia homeodomain is receptor-independent. J. Biol. Chem., 271: 18188-18193, 1996.

13. Giorello, L., Clerico, L., Pescarolo, M. P., Vikhanskaya, F., Salmona, M., Colella, G., Bruno, S., Mancuso, T., Bagnasco, L., Russo, P. and Parodi, S. Inhibition of cancer cell growth and c-Myc transcriptional activity by a c-Myc helix 1-type peptide fused to an internalization sequence. Cancer Res., 58: 3654-3659, 1998.

14. Fahraeus, R., Lain, S., Ball, K. L. and Lane, D. P. Characterization of the cyclin-dependent kinase inhibitory domain of the INK4 family as a model for a synthetic tumor suppressor molecule. Oncogene, 16: 587-596, 1998.

15. Mutoh, M., Lung, F. D., Long, Y. Q., Roller, P. P., Sikorski, R. S. and O'Connor, P. M. A $p21^{Waf1/Cip1}$ carboxyl-terminal peptide exhibited cyclin-dependent kinase-inhibitory activity and cytotoxicity when introduced into human cells. Cancer Res., 59: 3480-3488, 1999.

16. Jang, Y.-J., Lin, C.-Y., Ma, S. and Erikson, R. L. Functional studies on the role of the C-terminal domain of mammalian polo-like kinase. Proc. Natl. Acad. Sci., USA, 99: 1984-1989, 2002

17. Lane, H. A. and Nigg, E. A. Antibody microinjection reveals an essential role for human polo-like kinase 1 (Plk1) in the functional maturation of mitotic centrosomes. J. Cell Biol., 135: 1701-1713, 1996.

18. Cogswell, J. P., Brown, C. E., Bisi, J. E. and Neill, S. D. Dominant-negative polo-like kinase 1 induces mitotic catastrophe independent of cdc25C function. Cell Growth Differ., 11: 615-623, 2000.

19. Conn, C. W., Hennigan, R. F., Dai, W., Sanchez, Y. and Stambrook, P. J. Incomplete cytokinesis and induction of apoptosis by overexpression of the mammalian polo-like kinase, Plk3. Cancer Res., 60: 6826-6831, 2000.

20. Xie, S., Wu, H., Wang, Q., Cogswell, J. P., Husain, I., Conn, C.,

Stambrook, P., Jhanwar-Uniyal, M. and Dai, W. Plk3 functionally links DNA damage to cell cycle arrest and apoptosis at least in part via the p53 pathway. J. Biol. Chem., 276: 43305-43312, 2001.

Figure Legends

Fig. 11. (A) Alignment of the polo-boxes from Plk1, Plk2 (Snk) and Plk3 (Fnk/Prk). Conserved amino acids are shown in bold. Mutations are underlined. **(B)** Wild-type polo-box P1 and mutated polo-box P2 internalized into cells efficiently. MCF-7 and HeLa S3 cells were treated with FITC-labeled P1 (a, e, c and g) or P2 (b, f, d and h) for 3 h and visualized using a CSLM. a-d: images of phase-contrast (40x). e-h: use of FITC-labeled peptides (40x). **(C)** Wild-type polo-box P1 exerts its inhibitory effect on proliferation in a dose dependent manner. MCF-7 cells were incubated with indicated concentrations of wild-type polo-box P1 on day 1 and 3. Cells were counted on day 3 and 7. Results were based on two independent experiments (mean and SEM).

Fig. 12. Wild-type polo-box exhibited an antiproliferative activity on MCF-7 **(A)**, Saos-2 **(B)** and HeLa S3 cells **(C)**. Cells were treated with 5 μM of indicated peptides on day 1, 3, 6 and 8, harvested and counted on day 3, 6, 8 and 10. Values represent mean +/- SEM of 3 independent experiments. **(D)** G_2/M population was increased 25-35% after treatment with the polo-box. FACS analysis of HeLa S3 cells on day 6: Cells were treated as described in **(A-C)** and analyzed with Cycle TEST™ PLUS DNA reagent kit (Becton Dickson). **(E)** The number of mitotic cells increased 3-4 fold after treatment compared to control cells. HeLa S3 cells were treated 24 h with different peptides at 5 μM and stained for DNA and α-tubulin for subsequent fluorescence analysis. To determine the percentage of the mitotic population 500 cells were inspected. Each experiment was repeated three times independently.

Fig. 13. Wild-type polo-box induced apoptosis in MCF-7 and HeLa S3 cells. MCF-7 **(A)** and HeLa S3 **(B)** cells were treated for 16 h, stained with annexin V and PI, and analyzed using a flow cytometer. Camptothecin treatment (10 μM) served as positive control. **(C)** Cells were treated for 1 day, stained with Hoechst 33342 and visualized with a fluorescence

microscope (Leica). Upper panel: HeLa S3 cells treated with P1 and P3 (b-e), lower panel: MCF-7 (g-j). **(D)** Wild-type polo-box induced the misalignment of chromosomes and centrosomal abnormalities. Cells treated with peptides were further analyzed using DNA (a-c) or α-tubulin staining (d-f).

Fig. 14. Wild-type polo-box inhibited phosphorylation of substrates by Plk1 in vitro. Plk1 purified from Sf 9 cells was incubated with specific substrates at different concentrations of P1-P3 at 37°C for 20 min. **(A)** Autoradiogram of phosphorylated substrates. **(B)** Input control (Coomassie staining) **(C)** Standardized phosphorylation using a gel documentation system (Kodak).

Claims

1. Double stranded RNA (dsRNA) which is directed against PLK1.

2. Phosphorothioate antisense nucleotides (ASO) as described herein.

3. Inhibitory peptide as described herein.

4. Use of antisense oligonucleotides and/or double stranded RNAs and/or inhibitory peptide as claimed in claims 1, 2 or 3 for the inhibition of proliferative diseases .

5. Pharmaceutical composition for the treatment of proliferative diseases, especially cancer, containing an effective amount of a dsRNA and/or an ASO and/or an inhibitory peptide according to any one of claims 1 to 3.

Abstract

The present invention concerns inhibition of the activity of PLK1, which seems to be connected with cancer growth. Duplex RNAs antisense oligonucleotides and inhibitory peptides have been found to be useful in such inhibition, therefor they are claimed as ingredients fo pharmaceutical compositions for the treatment of proliferative diseases, preferably cancer of various types.

cl 17.05.2002

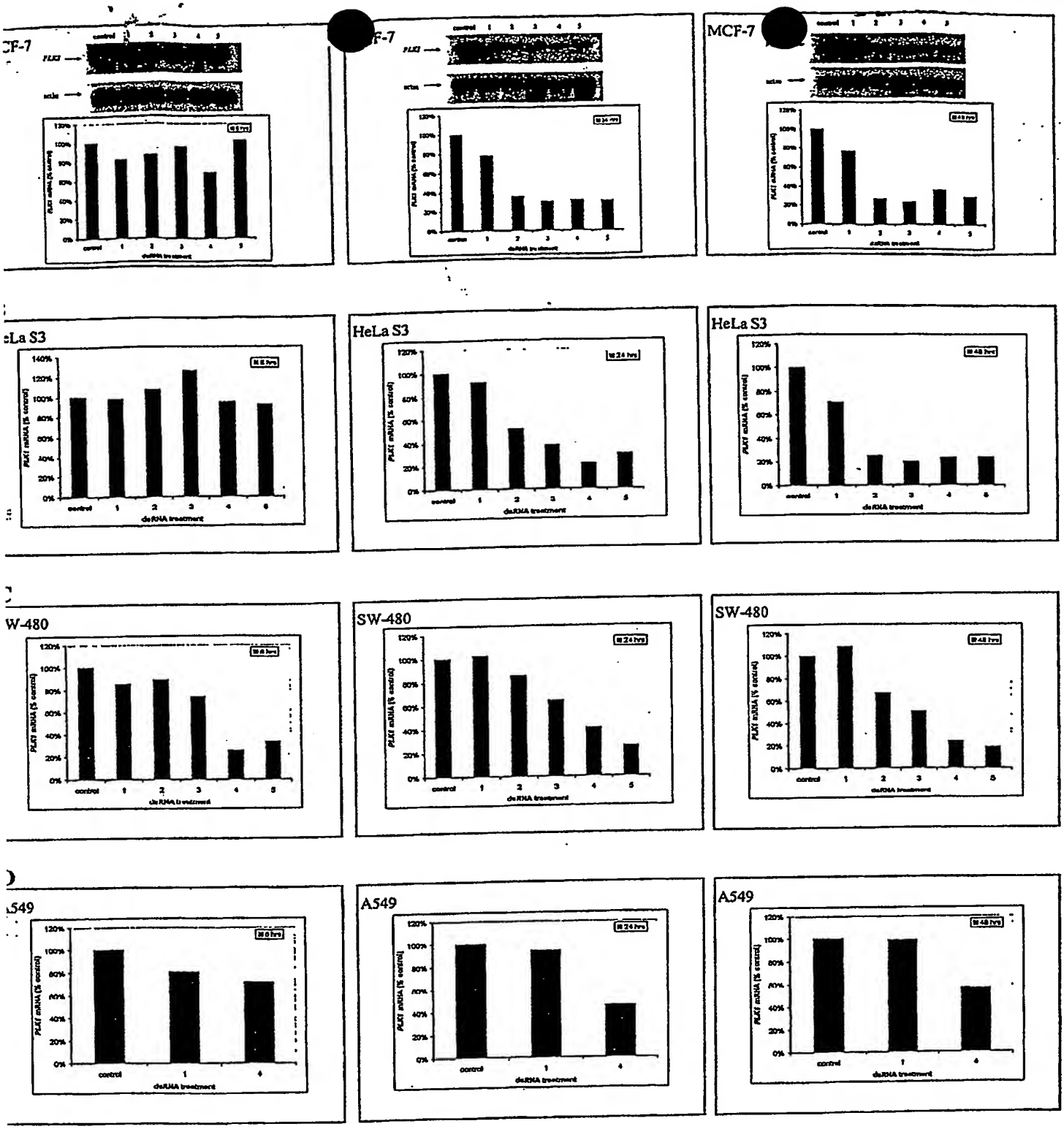
MCF-7
HeLa S3
HeLa S3
SW-480
SW-480
A549
A549
control
dsRNA treatment

Fig. 1

A

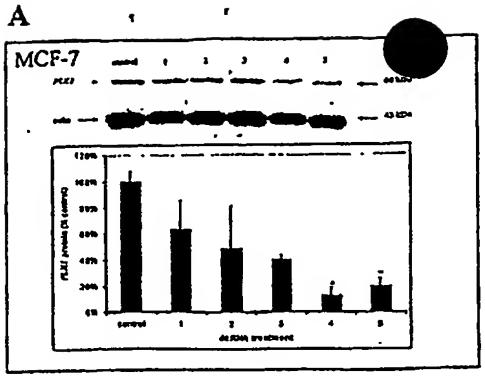
MCF-7
control
1
2
3
4
5
PLK1 protein (% control)
dsRNA treatment

B

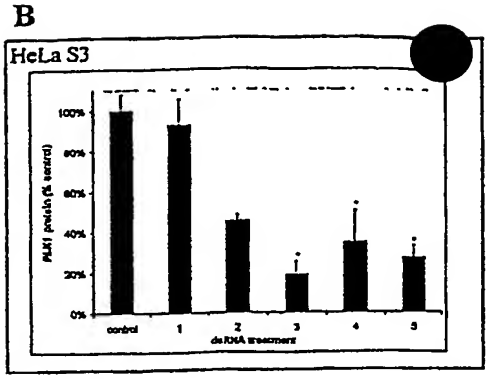
HeLa S3
100%
80%
60%
40%
20%
0%
control
1
2
3
4
5
dsRNA treatment

C

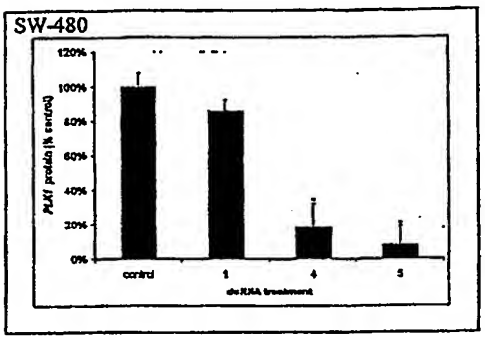
SW-480
120%
100%
80%
60%
40%
20%
0%
PLK1 protein (% control)
control
1
4
5
dsRNA treatment

D

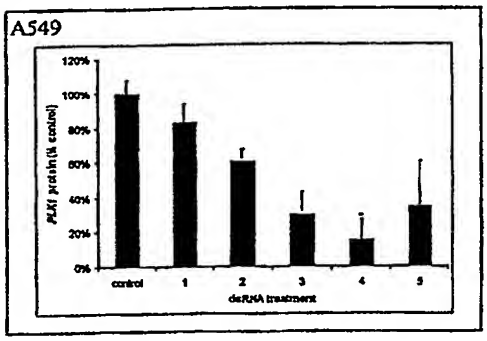
A549
120%
100%
80%
60%
40%
20%
0%
PLK1 protein (% control)
control
1
2
3
4
5
dsRNA treatment

E

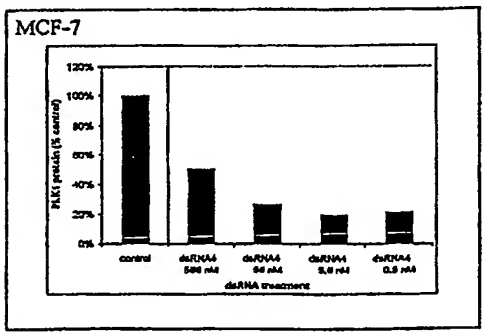
MCF-7
120%
100%
80%
60%
40%
20%
0%
control
dsRNA4
dsRNA4
dsRNA4
dsRNA4
dsRNA treatment

Fig. 2

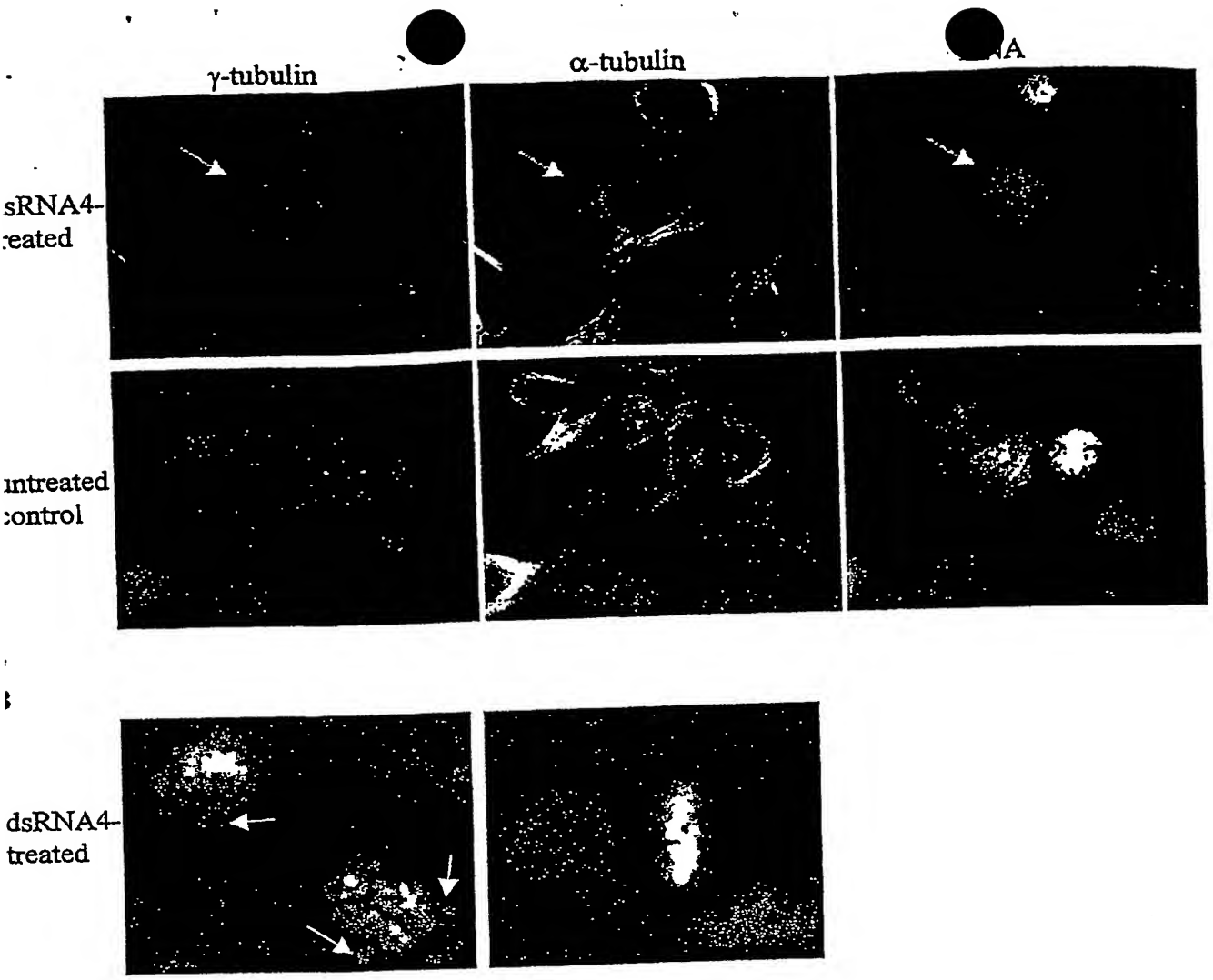
γ-tubulin
α-tubulin
sRNA4-
eated
ntreated
ontrol
dsRNA4-
treated

Fig. 3

A

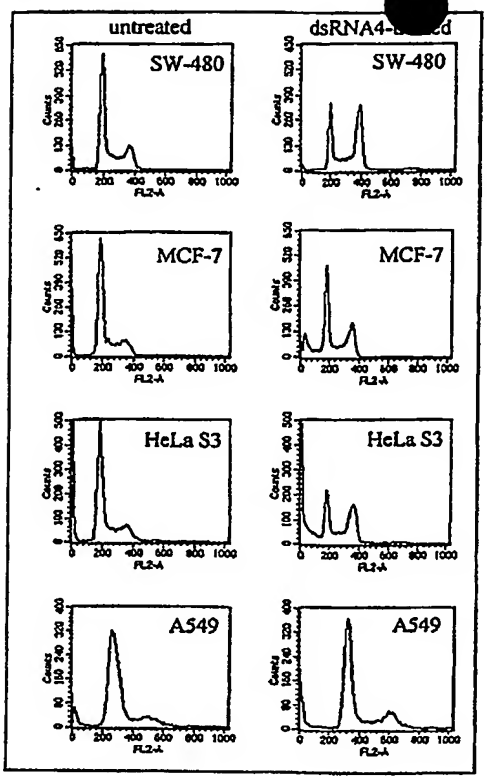
untreated
dsRNA4-treated
SW-480
SW-480
MCF-7
MCF-7
HeLa S3
HeLa S3
A549
A549

B

Fig. 4

A

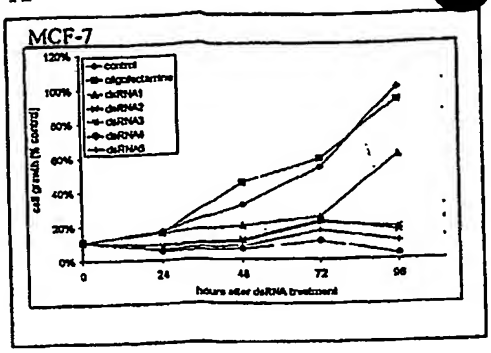
MCF-7
control
oligofectamine
dsRNA1
dsRNA2
dsRNA3
dsRNA4
dsRNA5
cell growth (% control)
hours after dsRNA treatment

B

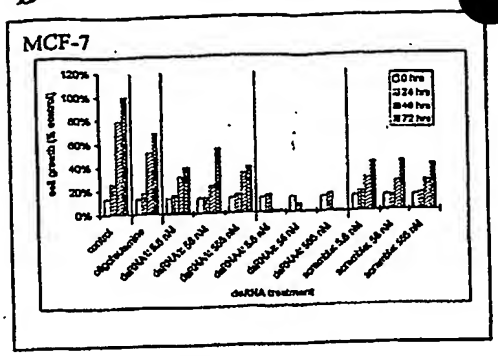
MCF-7
0 hrs
24 hrs
48 hrs
72 hrs
cell growth (% control)
control
oligofectamine
dsRNA1: 5.6 nM
dsRNA2: 56 nM
dsRNA3: 560 nM
dsRNA4: 5.6 nM
dsRNA5: 56 nM
dsRNA5: 560 nM
scramble: 5.6 nM
scramble: 56 nM
scramble: 560 nM
dsRNA treatment

C

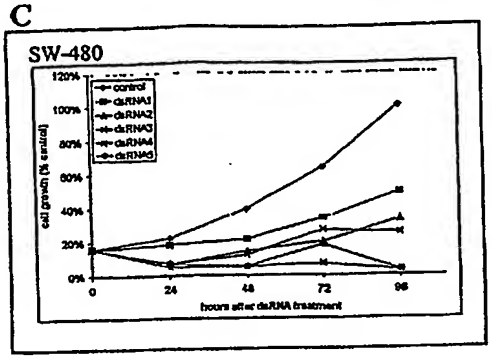
SW-480
control
dsRNA1
dsRNA2
dsRNA3
dsRNA4
dsRNA5
cell growth (% control)
hours after dsRNA treatment

D

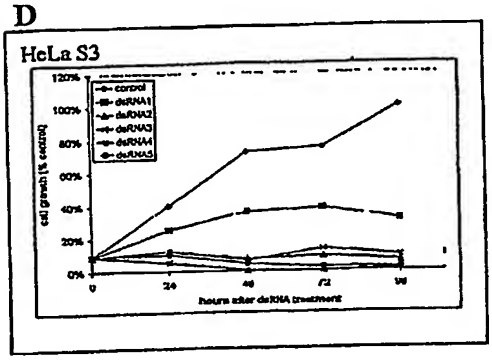
HeLa S3
control
dsRNA1
dsRNA2
dsRNA3
dsRNA4
dsRNA5
cell growth (% control)
hours after dsRNA treatment

E

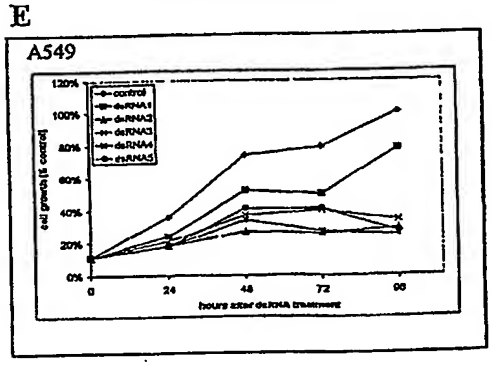
A549
control
dsRNA1
dsRNA2
dsRNA3
dsRNA4
dsRNA5
cell growth (% control)
hours after dsRNA treatment

F

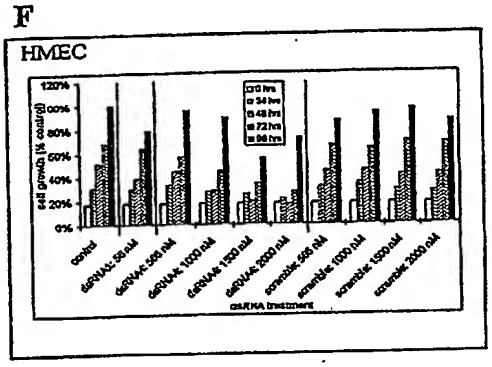
HMEC
0 hrs
24 hrs
48 hrs
72 hrs
96 hrs
cell growth (% control)
control
dsRNA1: 56 nM
dsRNA4: 560 nM
dsRNA5: 1000 nM
dsRNA5: 1500 nM
dsRNA5: 2000 nM
scramble: 560 nM
scramble: 1000 nM
scramble: 1500 nM
scramble: 2000 nM
dsRNA treatment

Fig. 5

a

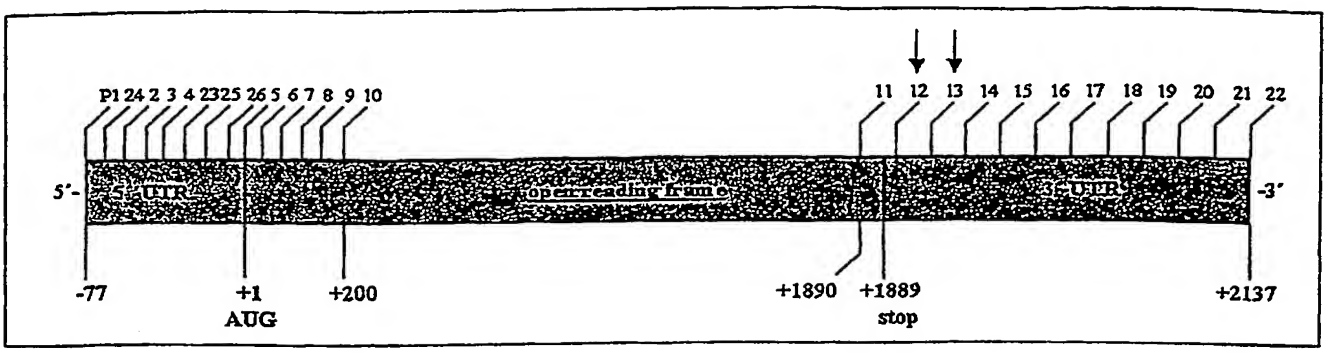
P1 24 2 3 4 2325 26 5 6 7 8 9 10
11 12 13 14 15 16 17 18 19 20 21 22
5'-
5' UTR
-3'
-77
+1
AUG
+200
+1890
+1889
stop
+2137

b

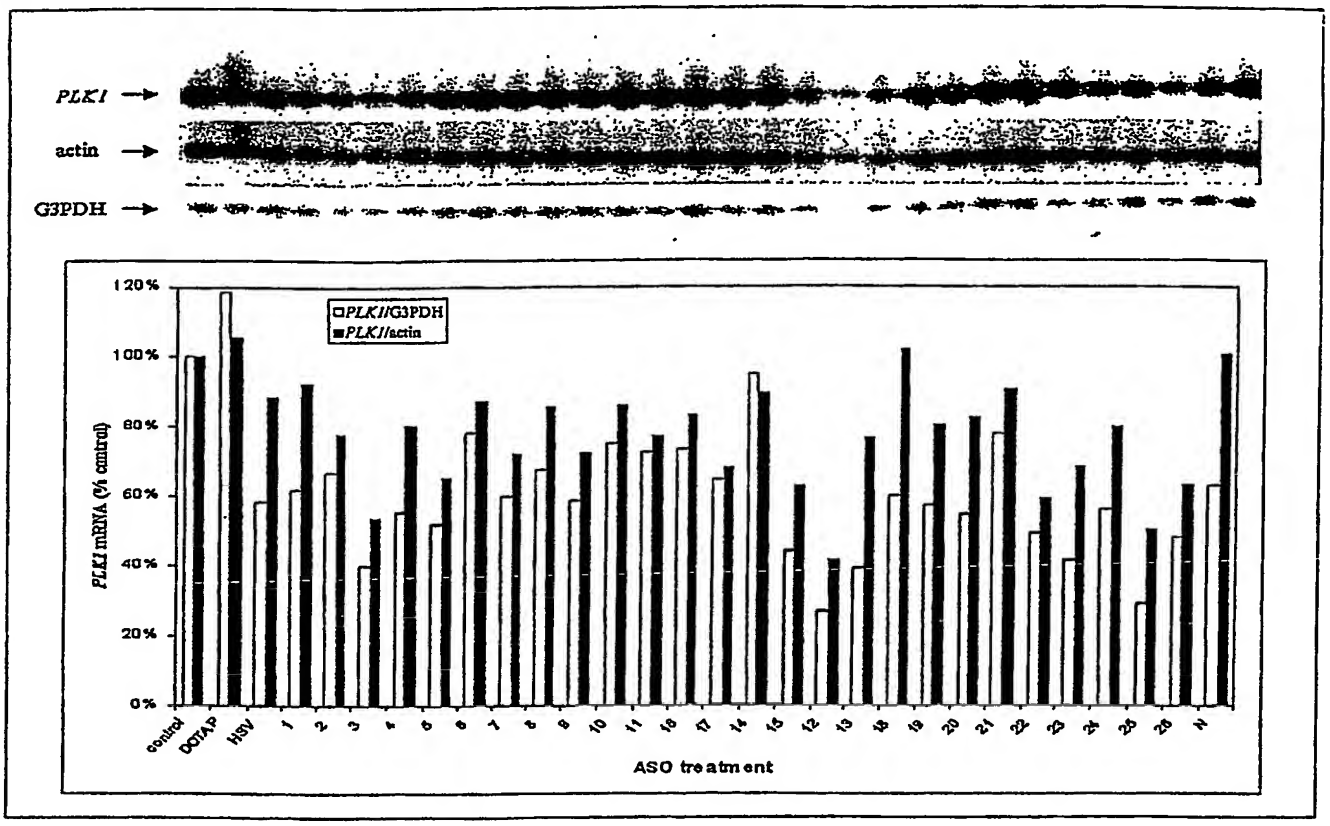
PLK1
actin
G3PDH
PLK1/G3PDH
PLK1/actin
PLK1 mRNA (% control)
120%
100%
80%
60%
40%
20%
0%
control
DOTAP
HSV
ASO treatment

c

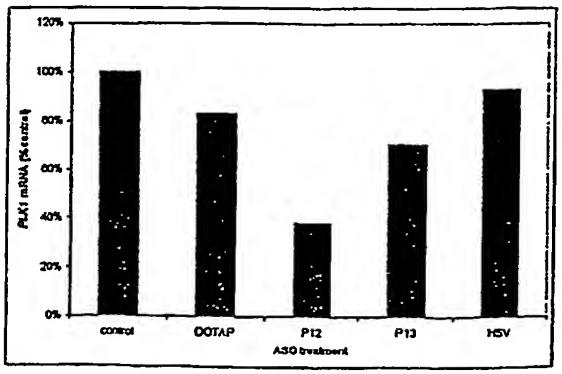
control
DOTAP
P12
P13
HSV
ASO treatment

d

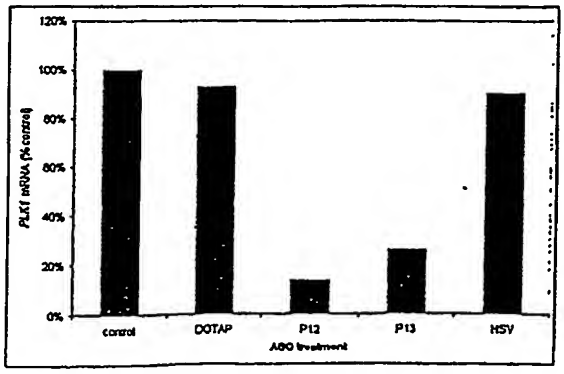
control
DOTAP
P12
P13
HSV
ASO treatment

Fig. 6

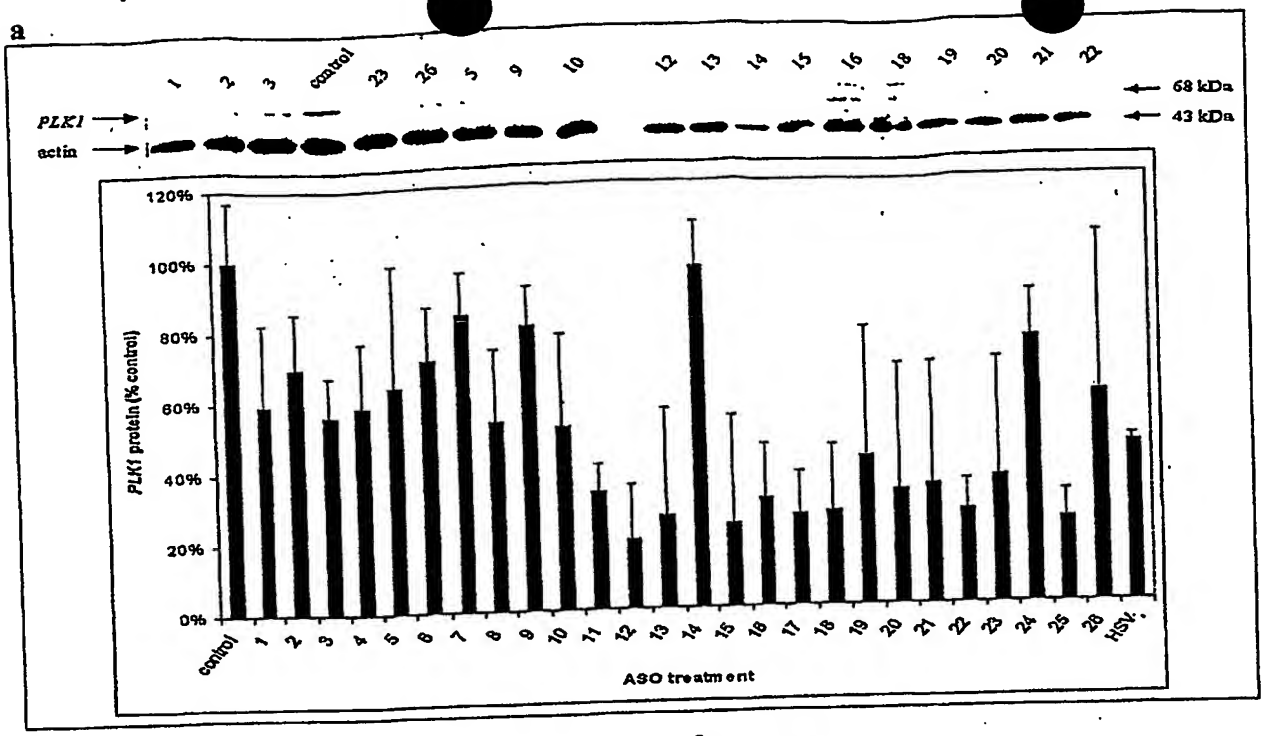
a
1 2 3 control 23 25 5 9 10 12 13 14 15 16 18 19 20 21 22
68 kDa
43 kDa
PLK1
actin
PLK1 protein (% control)
120%
100%
80%
60%
40%
20%
0%
control 1 2 3 4 5 6 7 8 9 10 11 12 13 14 15 16 17 18 19 20 21 22 23 24 25 26 HSV
ASO treatment

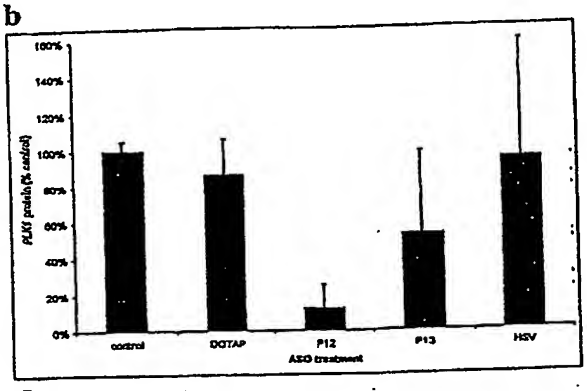
b
PLK1 protein (% control)
control
DOTAP
P12
P13
HSV
ASO treatment

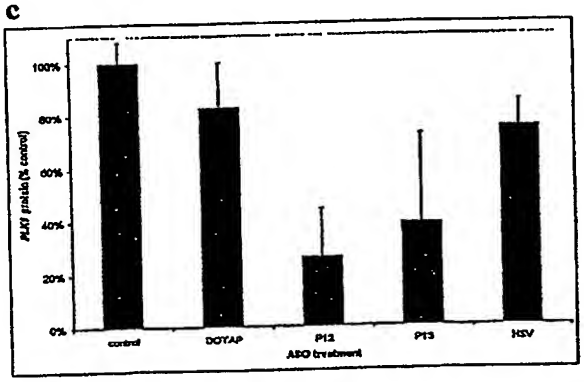
c
PLK1 protein (% control)
control
DOTAP
P12
P13
HSV
ASO treatment

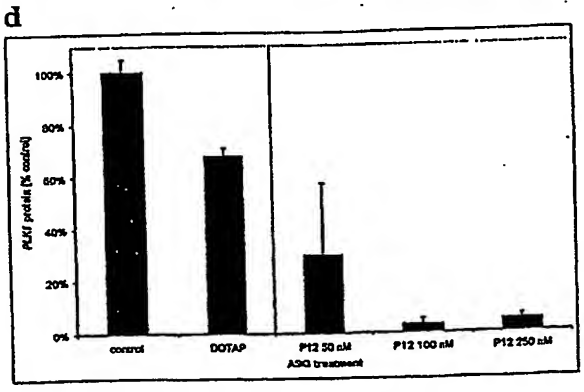
d
PLK1 protein (% control)
control
DOTAP
P12 50 nM
P12 100 nM
P12 250 nM
ASO treatment

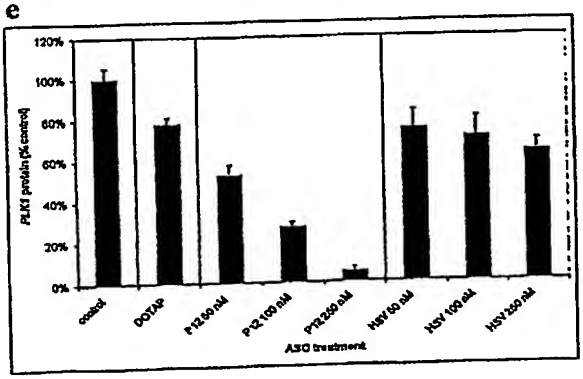
e
PLK1 protein (% control)
control
DOTAP
P12 50 nM
P12 100 nM
P12 250 nM
HSV 50 nM
HSV 100 nM
HSV 250 nM
ASO treatment

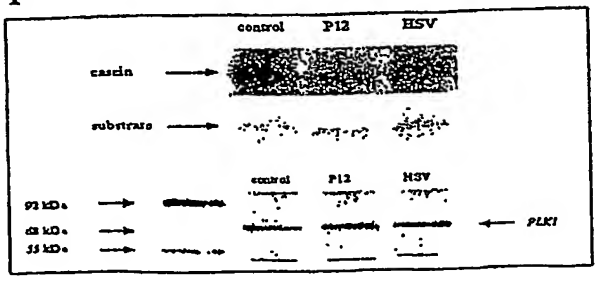
f
control
P12
HSV
casein
substrate
control
P12
HSV
92 kDa
PLK1

Fig. 7

a

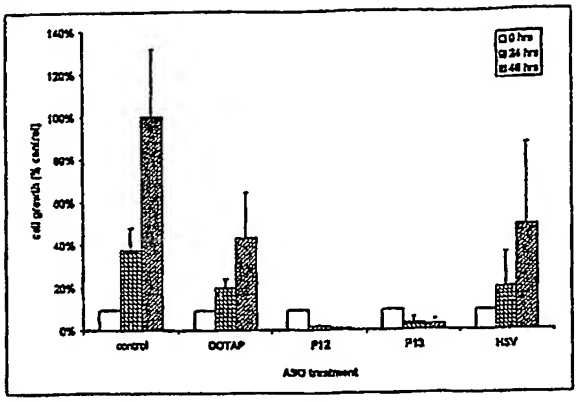
0 hrs
24 hrs
48 hrs
cell growth (% cont/ml)
control
DOTAP
P12
P13
HSV
ASO treatment

b

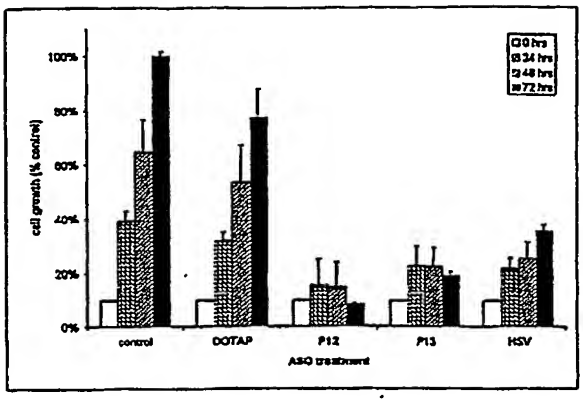
0 hrs
24 hrs
48 hrs
72 hrs
cell growth (% control)
control
DOTAP
P12
P13
HSV
ASO treatment

c

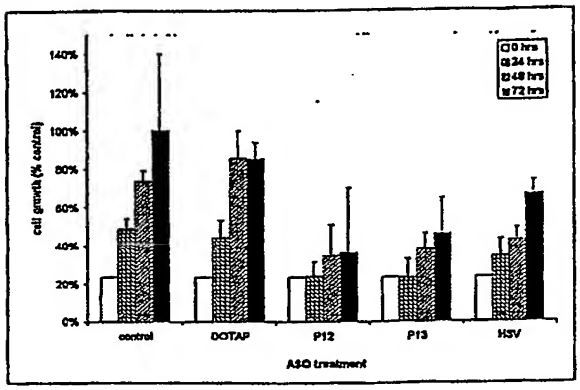
0 hrs
24 hrs
48 hrs
72 hrs
cell growth (% cont/ml)
control
DOTAP
P12
P13
HSV
ASO treatment

d

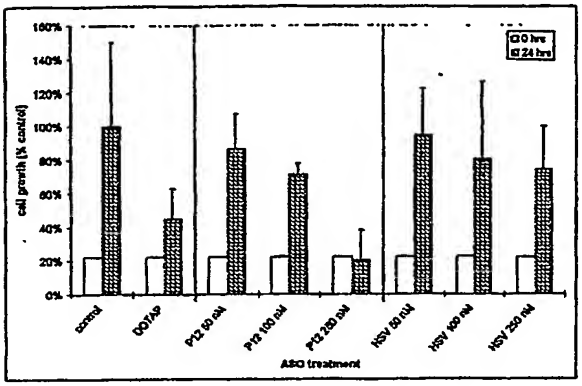
0 hrs
24 hrs
cell growth (% control)
control
DOTAP
P12 50 nM
P12 100 nM
P12 200 nM
HSV 50 nM
HSV 100 nM
HSV 250 nM
ASO treatment

e

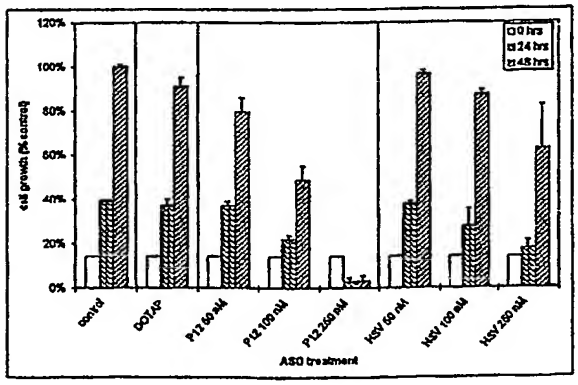
0 hrs
24 hrs
48 hrs
cell growth (% control)
control
DOTAP
P12 50 nM
P12 100 nM
P12 200 nM
HSV 50 nM
HSV 100 nM
HSV 250 nM
ASO treatment

Fig. 8

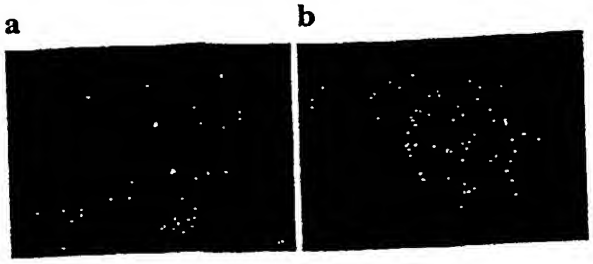

Fig. 5

a

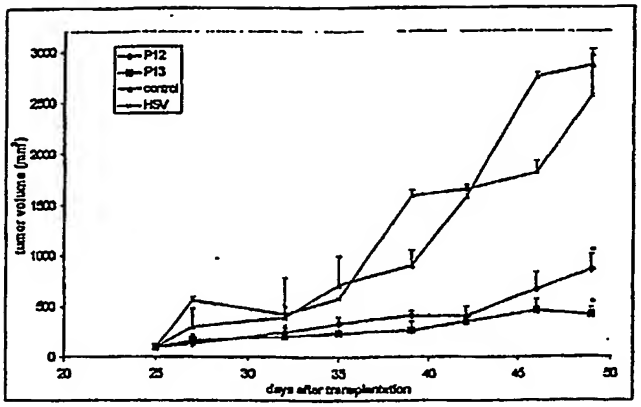
P12
P13
control
HSV
tumor volume (mm³)
3000
2500
2000
1500
1000
500
0
20
25
30
35
40
45
50
days after transplantation

b

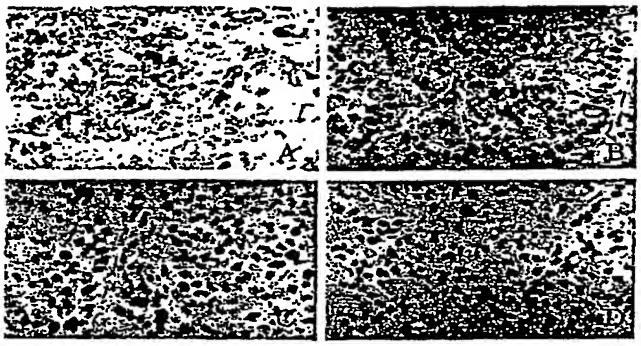
A
B
C
D

Fig. 10

Fig. 14

A

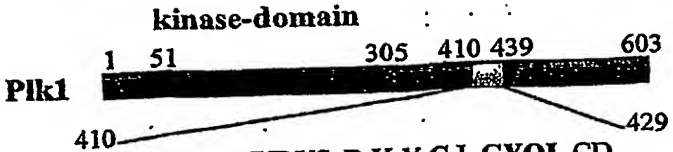

Plk1 WV S KWVDYS D K Y G L GYQL CD

Plk2 WV T KWVDYS N K Y G F GYQL DH

Plk3 WV S KWVDYS N K F G F GYQL SS

P1 WVSKWVDYSDKYGLGYQLCD- 16-mer

P2 WVSKFADYSDKYGAGYQLCD - 16-mer

P3 16-mer (Antennapedia)

B

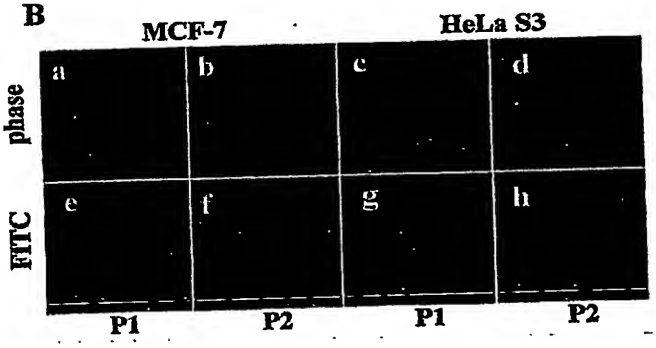

C

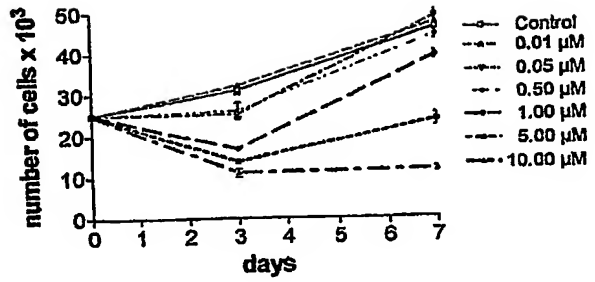

Fig 2

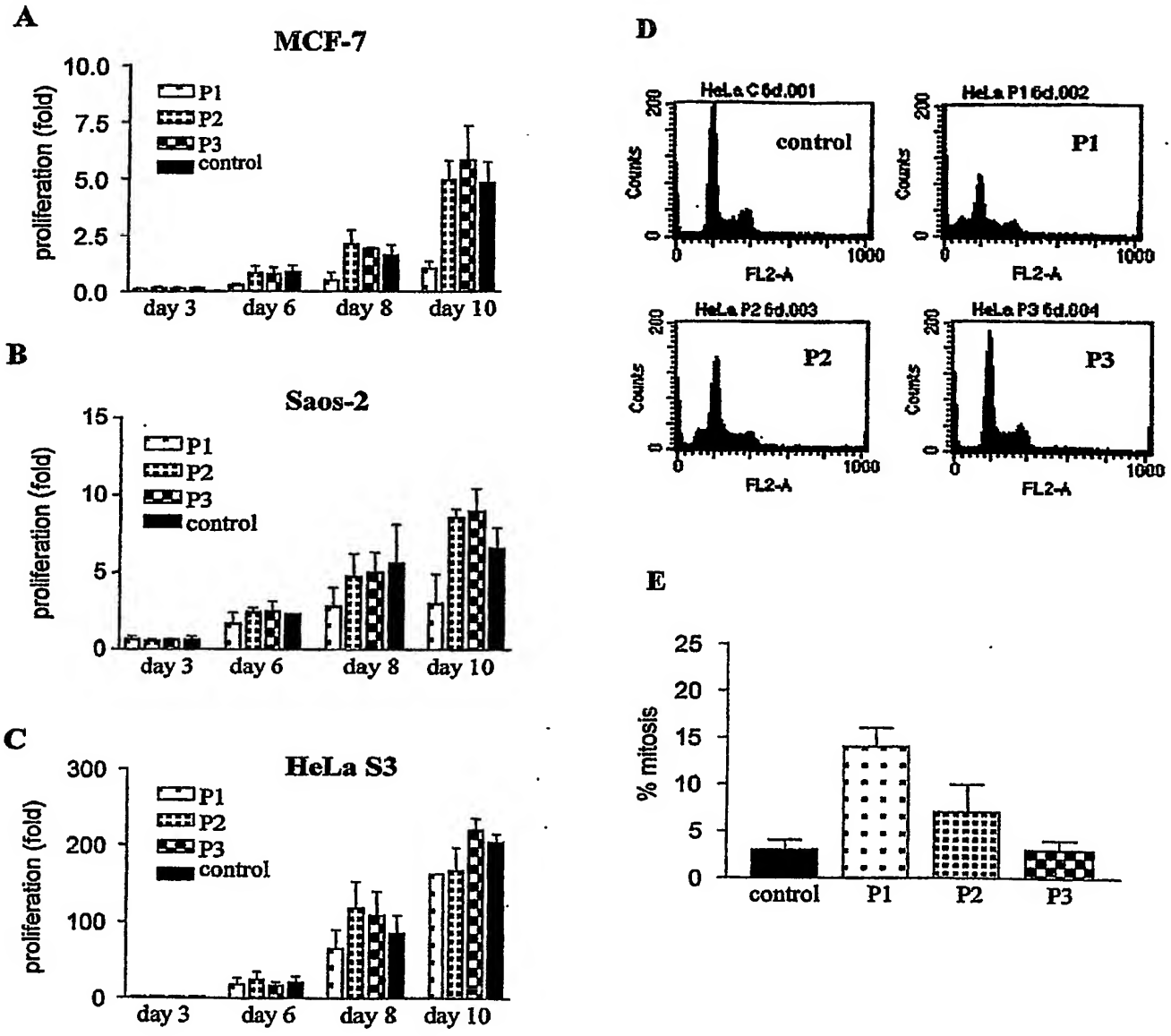
A
MCF-7
proliferation (fold)
10.0
7.5
5.0
2.5
0.0
P1
P2
P3
control
day 3
day 6
day 8
day 10
B
Saos-2
proliferation (fold)
15
10
5
0
C
HeLa S3
proliferation (fold)
300
200
100
0
D
HeLa C 6d.001
control
HeLa P1 6d.002
P1
HeLa P2 6d.003
P2
HeLa P3 6d.004
P3
Counts
FL2-A
E
% mitosis
25
20
15
10
5
0
control
P1
P2
P3

Fig. 3

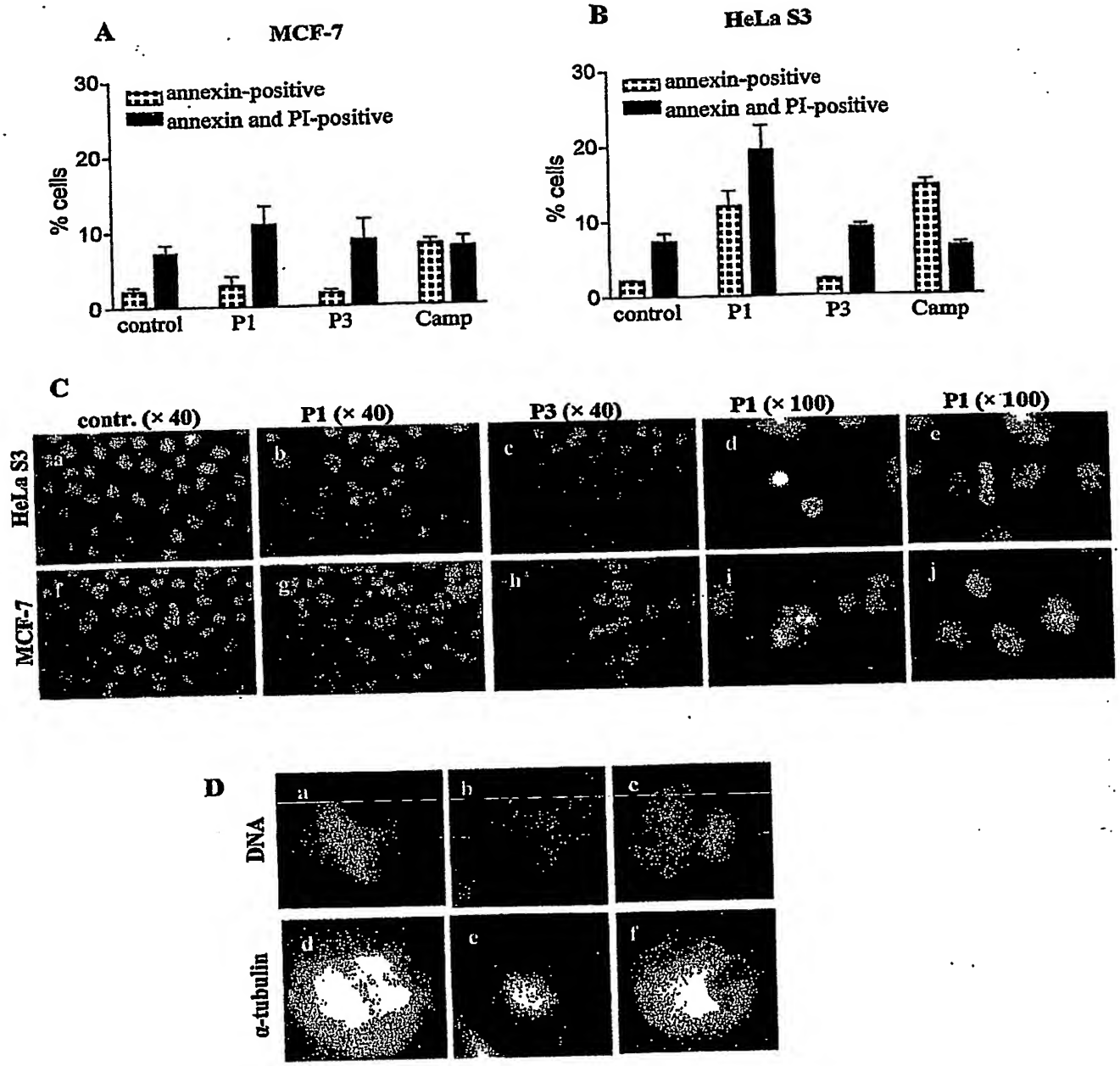
A
MCF-7
annexin-positive
annexin and PI-positive
% cells
30
20
10
0
control
P1
P3
Camp
B
HeLa S3
annexin-positive
annexin and PI-positive
% cells
30
20
10
0
control
P1
P3
Camp
C
contr. (× 40)
P1 (× 40)
P3 (× 40)
P1 (× 100)
P1 (× 100)
HeLa S3
MCF-7
a
b
c
d
e
f
g
h
i
j
D
DNA
α-tubulin
a
b
c
d
e
f

Fig.4

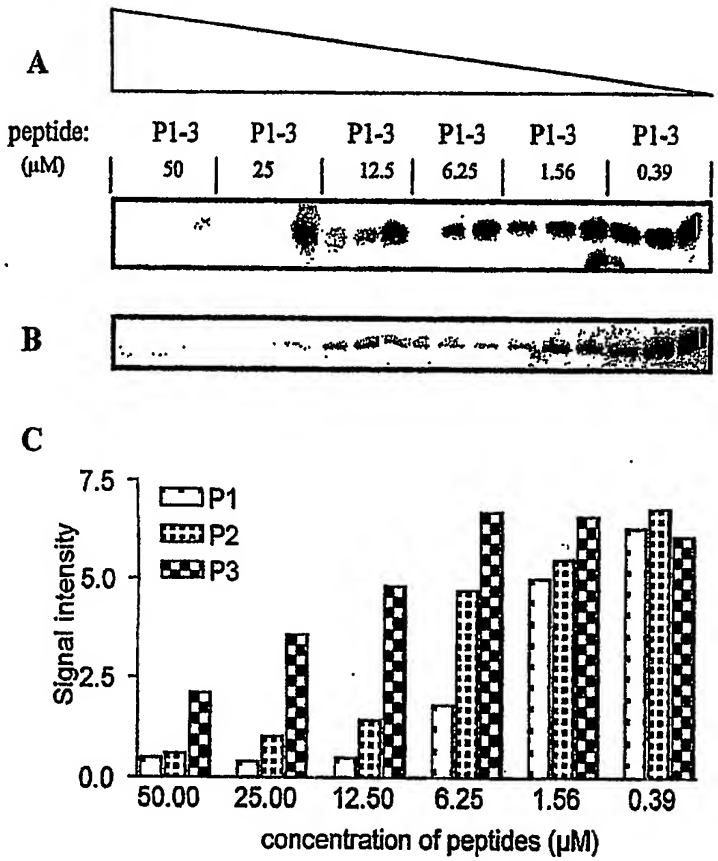
A
peptide:
(μM)
P1-3
50
P1-3
25
P1-3
12.5
P1-3
6.25
P1-3
1.56
P1-3
0.39
B
C
7.5
5.0
2.5
0.0
Signal intensity
P1
P2
P3
50.00
25.00
12.50
6.25
1.56
0.39
concentration of peptides (μM)